

Gliding performance is positively affected by the cranial movement of the abdominal organs

(水泳パフォーマンスは体幹内臓器の頭側移動により好影響を受ける)

東北大学大学院医学系研究科 医科学専攻

機能医科学講座 内部障害学分野

吉田直記

TABLE OF CONTENTS

	Page
I . SUMMARY	3
II . BACKGROUND	5
III . PURPOSE	10
IV . MATERIALS AND METHODS	11
V . RESULTS	18
VI . DISCUSSION	24
VII . CONCLUSION	34
VIII . REFERENCES	35
IX . ACKNOWLEDGEMENTS	40
X . FIGURES	41

I. SUMMARY

Background: Swimming is an extremely popular sport worldwide. The streamlined body position is a crucial and foundational position for swimmers. Because the density of the lungs is low, the center of buoyancy is always on the cranial side, and the center of gravity is always on the caudal side. Prior studies reported that the greater the distance between the centers of buoyancy and gravity, the more the swimmer's legs will sink, which is disadvantageous to swimming performance. However, how to reduce the distance between the centers of buoyancy and gravity has yet to be elucidated. On the other hand, in humans, the abdominal cavity is large and contains many organs. Previous studies have reported that, depending on posture, the location of these heavy abdominal organs can change in the abdomen. Hence, we hypothesized that a swimmer with high swimming performance can move their abdominal organs to the cranial side of the abdominal cavity, thus reducing the distance between the centers of buoyancy and gravity.

Objective: To evaluate the relationship between gliding performance and cranial movement of the abdominal organs in the streamlined body position of swimming.

Methods: Participants included 17 male college swimmers. The gliding distances

of the participants in the streamlined body position were measured in a pool, and participants were divided into two groups based on the measurements. In the high-performance group, the average gliding distance was >10 m, whereas in the low-performance group, the average gliding distance was <10 m. Magnetic resonance imaging measurements were taken with participants in a resting position and in a prescribed streamlined body position. To examine the shape of the abdominal cavity, the cross-sectional area (CSA) was measured at three levels along the torso: the upper liver level, lower lung level, and umbilical level.

Results: As compared with the low-performance group, the CSAs in the high-performance group increased significantly at the upper liver and lower lung levels and decreased significantly at the umbilical level.

Conclusion: Swimmers with high gliding performance exhibit different abdominal cavity shapes in the streamlined body position, which causes cranial movement of the abdominal organs. This movement can reduce underwater torque, prevent the legs from sinking during swimming, and have a positive effect on swimming performance.

II. BACKGROUND

In swimmers, the streamlined body position is a crucial and foundational position; furthermore, gliding ability plays an important role in race performance.¹⁾ In the streamlined body position, the swimmer places one hand over the other, with their fingers overlapping; raises their arms above their head; straightens their legs; and plantar flexes their feet.^{2, 3)} Swimming is one of the most challenging locomotion techniques for humans, and achieving a streamlined body position is important for improving swimming performance.^{4, 5)} The glide phase occurs when the swimmer attempts to travel through the water while maintaining the streamlined body position and taking no other action.^{6, 7)} The distance traveled during glide intervals is one indicator of gliding performance.^{6, 8)} This is significantly affected by drag, as swimming is performed in water, which has a greater density than air.^{1, 4, 9-11)} If the swimmer is being towed or is gliding, with no limb movement, the drag force is referred to as “passive drag,” whereas it is considered “active drag” when the swimmer is propelling themselves.^{5, 12-15)} Hence, to improve gliding performance, passive drag must be reduced.

Two forces in the water act upon the streamlined body position: buoyancy force

and gravity force.¹⁶⁾ Because the chest contains the air-filled lungs, which have a lower density than the surrounding water, the center of buoyancy is located here, on the cranial side of the torso, whereas the center of gravity is always on the caudal side.¹⁷⁾ When submerged, an object will rotate until the centers of buoyancy and gravity are aligned vertically. In the human body, this rotation that occurs in the streamlined body position causes the legs to sink^{18, 19)} (**Figure 1**). This has been studied as underwater torque, which is one of the main factors that increases drag in swimming.¹⁹⁻²¹⁾ A previous study found that the greater the distance between the centers of buoyancy and gravity, the greater the underwater torque.²²⁾ Thus, to reduce the effects of drag, it is important to investigate ways to reduce the distance between the centers of buoyancy and gravity in the streamlined body position. Some swimmers are able to maintain their legs afloat in the streamlined body position without any significant action (e.g., kicking; **Figure 2**). As shown in the photos in Figure 2, these swimmers use their abdominal muscles to draw in the belly, which in turn causes the legs to float. This phenomenon can be explained by the abdominal contraction that occurs, reducing the distance between the center of buoyancy and the center of gravity. Abdominal contraction can improve gliding performance because if the legs do not sink, the frontal surface area is reduced. As the frontal surface area decreases, there is a

decrease in the swimmer's drag.^{6, 23)} However, the mechanism underlying the reduced distance between the centers of buoyancy and gravity when the belly is drawn in has not yet been elucidated.

Pilot study

It has been reported that lumbar kyphosis and anterior pelvic tilt decrease in the streamline of skilled swimmers, but how these swimmers balance the center of gravity and center of buoyancy is still unclear. Previously, we conducted pilot studies to investigate the migration of internal abdominal organs in a streamlined body position during swimming using computed tomography (CT). We obtained CT images of a healthy asymptomatic male elite swimmer aged 28 years while he took both streamlined and nonstreamlined positions. Using an underwater camera, we confirmed that the swimmer could float in the pool in a streamlined position, but in the nonstreamlined position, he could not float, and his lower body sunk underwater. Using CT, we measured the migration of the internal abdominal organs, the thickness of the lateral abdominal wall muscles, lung shape, and the presence of lumbar lordosis. The lumbar lordosis was determined as the angle between Th12 and S1. In the sagittal view at the left kidney level, the maximum value of the anteroposterior system of the lung was defined as the anteroposterior

diameter. In the coronal view at the tracheal bifurcation, the vertical diameter was defined as the distance from the tracheal bifurcation to the left lung base. The CT results showed a migration of approximately two vertebral body distances to the head side in the liver, kidney, and spleen in the streamlined position (**Figure 3**). Furthermore, the anteroposterior diameter of the lung increased from 156 mm to 166 mm, and the vertical diameter decreased from 217 mm to 151 mm (**Figure 4**). The lumbar lordosis decreased from 81° to 40° (**Figure 5**), and the lateral abdominal wall muscles (transversus abdominis [TrA], external oblique [EO], and internal oblique [IO]) increased from 17 mm to 31 mm (**Figure 6**). The results of this study suggested that when an elite swimmer is in a streamlined position, the internal abdominal organs move to the cranial side.

In humans, the abdominal cavity is large and contains many organs. The average weights of the abdominal organs in healthy males ($18.5 \text{ kg/m}^2 \leq \text{body mass index [BMI]} < 25 \text{ kg/m}^2$) are as follows: liver, 1414 g (range, 838–2013 g); right kidney, 121 g (range, 84–200 g); left kidney, 129 g (range, 93–201 g); and spleen, 127 g (range, 53–299 g).²⁴⁾ The densities of the abdominal organs are as follows: liver, 1.050 g/cm^3 ; right kidney, 1.050 g/cm^3 ; left kidney, 1.050 g/cm^3 ; and spleen, 1.040 g/cm^3 .²⁵⁾

The abdominal cavity also contains luminal organs, the weights of which are greatly affected by meals. Prior studies have reported that, depending on posture, these heavy abdominal organs can change their location in the abdomen.²⁶⁻²⁹⁾ Hence, we hypothesized that a swimmer with high gliding performance can move their abdominal organs to the cranial side of the abdominal cavity, thus reducing the distance between the centers of buoyancy and gravity.

III. PURPOSE

The aim of this study was to examine the relationship between gliding performance and cranial movement of the abdominal organs in the streamlined body position of swimming.

IV. MATERIALS AND METHODS

This prospective cohort study was conducted at Tohoku University Hospital in Japan. The study was approved by the ethics committee of Tohoku University (approval No. 15263), and all procedures were performed in accordance with the approved guidelines. All participants provided written informed consent.

Participants

For this study, we recruited consecutive healthy, male college swimmers between 20 and 30 years old, with a BMI of 18–25 kg/m². Swimmers were excluded if they experienced any pain in the streamlined body position, had neurologic or respiratory disorders, had contraindications to magnetic resonance imaging (MRI), such as claustrophobia, or were deemed by doctors as inappropriate for study participation. Seventeen male college swimmers participated in this study.

Measurements on land

An experienced physiotherapist measured the height, weight, upper extremity length, lower extremity length, and shoulder width of each participant. The upper extremity length was measured from the acromion process to the tip of the radial

styloid process. Lower extremity length was measured from the anterior superior iliac spine to the medial malleolus. Shoulder width was measured between the acromion processes. Body surface area (BSA) was calculated using the formulas of Du Bois³⁰ based on height and weight.

Gliding distance

We measured the gliding distance in the streamlined body position for each participant in an indoor pool (**Figure 7**). Gliding distance was defined as the maximum distance the swimmer could cover in the streamlined body position without any arm strokes or kicks. The pool was 25-m long, with a depth of 1.3 m. Participants wore standard swimsuits. They began by standing on the pool floor, then submerged and maximally pushed off the wall in the streamlined body position. The distance between the pool wall and the tip of the participant's hand was measured accurately when gliding ceased. This measurement was performed five times for each participant, and the average measurement was used to sort participants into two groups for comparison: the high-performance group, in which the average gliding distance was >10 m, and the low-performance group, in which the average gliding distance was <10 m.

MR examination

We performed the MR examinations using a 3.0-T whole-body MR scanner (Ingenia 3.0T, Philips Medical Systems, Best, the Netherlands) with a 32-channel torso coil. Participants were placed in the prone position with their hands up and overlapping, head between the extended arms, and feet together and plantar flexed (**Figure 8**). To enable the prone position to be held without difficulty, a soft cushion was used on the ventral side. MR scans were performed in both the resting and streamlined body positions.

Streamlined body position: Participants were instructed to maintain the streamlined body position as if underwater, inhale, and hold their breath.

Resting position: Participants were instructed to relax their body, inhale the same amount of air as they had in the streamlined body position, and hold their breath.

The participants determined the volume of air intake, provided that air intake in the resting position was equal to that in the streamlined body position using auto voice. Two-dimensional (2D) turbo-spin echo T2-weighted images were acquired in sagittal orientations with repetition time (TR) = 2441 ms, echo time (TE) = 135 ms, flip angle (FA) = 90°, slice thickness = 4 mm, acquisition matrix = 380 × 225, and field of view = 38 × 38 cm. Three-dimensional (3D) T1-weighted fast-field echo (enhanced T1 high-resolution isotropic volume excitation [eTHRIVE], Philips

Medical Systems) images were acquired in coronal orientations with TR = 3.7 ms, TE = 1.8 ms, FA = 10°, slice thickness = 4 mm, field of view = 50 × 50 cm. The 2D T2-weighted and 3D T1-weighted images were acquired to cover the body trunk in two stations. Each MRI scan was performed within 20 seconds, during which the participants held their breath. The multistation images were combined into a single full-field view on the MR console (MR MobiView, Philips Medical Systems).

MR image analysis

We analyzed the MR images using a commercially available workstation (Ziostation2; Ziosoft, Tokyo, Japan). The acquired T1-weighted images were reconstructed into axial images. To evaluate the cranial movement of abdominal organs, the cross-sectional area (CSA) of the abdominal cavity was measured at three levels: upper liver level, lower lung level, and umbilical level. The retroperitoneal space was included in the CSA in this study, but the aorta and inferior vena cava were excluded because they were relatively fixed. Furthermore, we measured the maximum thickness of the rectus abdominis muscle (RA) and the anterolateral abdominal wall, which was composed of the TrA, EO, and IO, at the umbilical level (TrA + EO + IO). Muscle thicknesses were measured on both right and left sides, and an average value for each was calculated (**Figure 9**). To

further investigate the changes in abdominal cavity shape, the ratios of CSA at the upper liver and lower lung levels to the umbilical level were calculated in the resting position and streamlined body position.

Center of gravity

The center of gravity is an imaginary point through which the gravitational force acts on an object.³¹⁾ To objectively measure the movement of the center of gravity from the resting to the streamlined body positions, we further recruited 10 of the 17 participants who underwent MRI. Five participants were from the high-performance group, and other five participants were from the low-performance group. We measured the center of gravity using the reaction board method,^{17, 32)} and ground reaction force data were acquired using 90 × 60-cm force plates (Anima Corporation, Chofu, Tokyo, Japan).³³⁾ Participants were placed on the balance board in the supine position, and measurements were performed in both the streamlined body position and resting position. For the streamlined body position, participants were instructed to hold a streamlined position as if underwater. For the resting position, participants were instructed to raise their arms above their head, as in the streamlined body position, and to relax their body (**Figure 10**).

The measurement point was at the tip of the finger, and the pivot point was at the soles of the feet (**Figure 11**). The center of gravity was calculated as follows:

$$CG = \frac{L \times RF}{W} \quad (1)$$

where CG is the distance from the feet to the participant's center of gravity, L is the length between the tip of the longest finger and the soles of the feet, RF is the reaction force at the tip of the finger (without the weight of the balance board itself), and W is the participant's weight. The movement of CG from the resting position to the streamlined body position (CGx) was calculated as follows:

$$CGx = CG1 - CG2 = \frac{L \times (RF1 - RF2)}{W} \quad (2)$$

where CG1 is the center of gravity in the streamlined body position, CG2 is the center of gravity in the resting position, RF1 is the reaction force in the streamlined body position, and RF2 is the reaction force in the resting position.

To perform comparisons between the participants, CGx was expressed as follows as a percentage (CGx%) of each participant's length between the tip of the longest finger and the soles of the feet:

$$CGx\% = \frac{100 \times CGx}{L} \quad (3)$$

Statistical analysis

We performed all statistical analyses using EZR (Saitama Medical Center, Jichi Medical University, Saitama, Japan),³⁴⁾ which is a graphical user interface for R (The R Foundation for Statistical Computing, Vienna, Austria). More precisely, it is a modified version of the R commander designed to add statistical functions frequently used in biostatistics. All continuous variables were presented as medians with interquartile ranges. The Mann–Whitney U test was used for between-group comparisons, and the Wilcoxon signed-rank test was used for within-group comparisons. Spearman’s rank correlation coefficient was used to measure the degree of association between gliding distance and other factors. All P values of <0.05 were considered statistically significant.

V. RESULTS

We found no significant difference in characteristics with regard to age, height, weight, BMI, BSA, upper limb length, lower limb length, and shoulder width between participants in the high-performance group and those in the low-performance group (**Table 1**). In addition, there were no significant differences observed in characteristics with regard to height, length between the tip of the longest finger and the soles of the feet, or BMI between participants in the high-performance group and those in the low-performance group in the center of gravity studies (**Table 2**).

CSA within-group comparisons

In the high-performance group, the CSA increased significantly from the resting to the streamlined body positions at the upper liver and lower lung levels and decreased significantly at umbilical level (Wilcoxon signed-rank test, $P < 0.01$, $P < 0.01$, and $P < 0.01$, respectively). In the low-performance group, the CSA increased significantly only at the upper liver level, and there were no significant changes at the lower lung and umbilical levels (Wilcoxon signed-rank test, $P = 0.027$, $P = 0.65$, and $P = 0.25$, respectively; **Table 3**). Furthermore, we measured the maximum

thickness of the RA and anterolateral abdominal wall, which is composed of the TrA, EO, and IO muscles, at the umbilical level (TrA + EO + IO). In both the high- and low-performance groups, the thickness of the TrA + EO + IO increased significantly from the resting to the streamlined body positions at the umbilical level (Wilcoxon signed-rank test, $P = 0.016$ and $P = 0.012$, respectively). However, in both the high- and low-performance groups, the thickness of the RA was not significantly altered (Wilcoxon signed-rank test, $P = 0.35$ and $P = 0.25$, respectively; **Table 3**).

Changes in the CSA between study groups

In the high-performance group, changes in the CSA from resting to streamlined body positions were as follows: upper liver level, 36.8 cm² (median, interquartile range: 28.7–67.3); lower lung level, 23.2 cm² (17.3–44.2); and umbilical level, –37.4 cm² (–47.4 to –24.9). In the low-performance group, the following changes occurred in the CSA when transitioning from the resting to streamlined body positions: upper liver level, 16.4 cm² (9.3–22.2); lower lung level, –5.1 cm² (–15.4 to 11.6); and umbilical level, –1.2 cm² (–18.1 to 0.75). The changes in the CSA were significantly greater in the high-performance group than in the low-performance group at all three levels: upper liver level, lower lung level,

umbilical level (Mann–Whitney U test, $P = 0.036$, $P < 0.01$, and $P < 0.01$, respectively; **Figures 12, 13, and 14; Table 4**). These changes in abdominal cavity shape can cause cranial-side movement of the abdominal organs.

Correlation between gliding distance and participant characteristics

We examined the correlation between gliding distance and participant characteristics (**Table 5**). The correlation coefficients were <0.7 for age, height, weight, BMI, BSA, upper limb length, lower limb length, and shoulder width. Conversely, the correlation coefficient was >0.7 for years of swimming practice (YSP) ($P < 0.01$) (**Figure 15**).

Correlation between gliding distance and changes in CSA

Moreover, we examined the correlation between gliding distance and changes in CSA. The correlation coefficients were 0.63 for the changes in CSA at the upper liver level ($P < 0.01$), 0.78 for the changes in CSA at the lower lung level ($P < 0.01$), -0.78 for the changes in CSA at the umbilical level ($P < 0.01$) (**Figures 16, 17, and 18, respectively; Table 6**).

Ratio of CSA at the umbilical level to other CSAs

To further investigate the correlation with CSA, the ratio of CSA at the upper liver level to CSA at the umbilical level and the ratio of CSA at the lower lung level to CSA at the umbilical level were calculated.

In the resting position, the ratios of CSA at the upper liver level to CSA at the umbilical level were 2.75 (2.62–2.93) in the high-performance group and 2.65 (2.45–2.97) in the low-performance group (Mann–Whitney U test, $P = 0.67$). In the streamlined body position, the ratios of CSA at the upper liver level to CSA at the umbilical level were 4.50 (3.49–5.38) in the high-performance group and 3.15 (2.78–3.28) in the low-performance group (Mann–Whitney U test, $P < 0.01$). In the resting position, the ratios of CSA at the lower lung level to CSA at the umbilical level were 1.98 (1.81–2.25) in the high-performance group and 2.04 (1.64–2.06) in the low-performance group (Mann–Whitney U test, $P = 0.74$). In the streamlined body position, the ratios of CSA at the lower lung level to CSA at the umbilical level were 3.22 (2.67 to 3.63) in the high-performance group and 2.18 (1.84 to 2.41) in the low-performance group (Mann–Whitney U test, $P < 0.01$) (**Table 7**).

Correlation between gliding distance and the ratio of CSA

We examined the correlation between gliding distance and the ratio of CSA. The ratio of CSA at the upper liver level to umbilical level was 0.072 ($P = 0.78$) in the

resting position and 0.78 ($P < 0.01$) in the streamlined body position. The ratio of CSA at the lower lung level to umbilical level was -0.16 ($P = 0.55$) in the resting position and 0.76 ($P < 0.01$) in the streamlined body position (**Figures 19, 20, 21, and 22, respectively; Table 8**).

Representative case presentation

To compare the characteristics of the high- and low-performance groups, we present two cases. Case 1 is a representative of the high-performance group, with a height of 1.80 m, weight of 79 kg, YSP of 8 years, and gliding distance of 13 m. From the resting position to the streamlined body position, CSA at the upper liver level changed from 354.3 to 437.9 cm², CSA at the lower lung level changed from 318.9 to 326.2 cm², and CSA at the umbilical level changed from 122.8 to 71.7 cm² (**Figure 23A, A'**). Case 2 is a representative case from the low-performance group; the swimmer's height was 1.67 m, weight 60 kg, YSP 1 year, and gliding distance 8 m. From the resting position to the streamlined body position, CSA at the upper liver level changed from 303.9 to 313.2 cm², CSA at the lower lung level changed from 230.6 to 245.1 cm², and CSA at the umbilical level changed from 113.8 to 112.5 cm² (**Figure 23B, B'**). Swimmers in the high-performance group (as shown in case 1) exhibited different abdominal cavity shapes in the streamlined body

position as compared with the low-performance group (as show in case 2), which can result in cranial-side movement of abdominal organs.

Movement of center of gravity

The median CGx% was 0.334 (interquartile range: 0.184–0.359) in the high-performance group and 0.079 (0.048–0.170) in the low-performance group.

As compared with the low-performance group, the CGx% was significantly greater in the high-performance group (Mann–Whitney *U* test, $P = 0.032$; **Table 2**).

VI. DISCUSSION

Cranial-side movement of the abdominal organs

To our knowledge, this is the first study to use MRI to analyze changes in abdominal cavity shape in the streamlined body position. Our results indicate that as compared with the low-performance group, the high-performance group experienced significant changes in CSA in the streamlined body position. Specifically, the CSA of the high-performance group increased at the upper liver and lower lung levels but decreased at the umbilical level in the streamlined body position. In the case of continuous variables, all heights (upper liver level, lower lung level, and umbilical level) were highly correlated with the gliding distance. Specifically, at the upper liver and lower lung levels, the higher the CSA increased from the resting position to the streamlined body position, the longer was the gliding distance. At the umbilical level, the longer the CSA decreased from the resting position to the streamlined body position, the longer was the gliding distance. This change in abdominal cavity shape may result in cranial-side movement of the abdominal organs (**Figure 23**). The major abdominal organs are heavy, and their density is higher than that of water. When these abdominal organs move to the cranial side in the streamlined body position, the center of

gravity accordingly shifts to the cranial side.

Movement of the center of gravity

The CGx% was a positive value, which indicates that the center of gravity moved cranially when the participants were instructed to assume the streamlined body position. Furthermore, the high-performance group exhibited a significantly greater movement of the center of gravity. The supine posture on land is different from the prone posture in water; however, these results are consistent with our MRI findings and also underpin our hypothesis. In other words, the cranial movement of the center of gravity is caused by the cranial movement of the abdominal organs and activated abdominal muscles. This movement of the center of gravity reduces the distance between the centers of buoyancy and gravity, resulting in decreased underwater torque.

Changes in abdominal cavity shape

To further investigate the changes in abdominal cavity shape, we calculated the ratios of CSA at the upper liver and lower lung levels to umbilical level in the resting position and streamlined body position. There was no significant difference in the ratio of CSA at the upper liver level to umbilical level and in the

ratio of CSA at the lower lung level to umbilical level between the high- and low-performance groups in the resting position, but there was a significant difference in both the ratios of CSA between the two groups in the streamlined body position (**Table 7**). In the streamlined body position, the two ratios and gliding distance were highly correlated (**Table 8**). In this study, we used a prone streamline posture, but we expect similar results with a supine streamline posture. Since the shape change is highly correlated with the kicking distance, it is expected that low-level players can also increase their kicking distance by training to change the shape. It is necessary to conduct intervention studies in the future to confirm these findings.

Underwater torque

One of the main effects of increasing the frontal surface area in the streamlined body position is underwater torque.³⁵⁾ As the increased frontal surface area leads to increased drag, swimmers aim to reduce their underwater torque.³⁶⁾ In the human body, the center of buoyancy is always on the cranial side, and the center of gravity is always on the caudal side.¹⁷⁾ The distance between the centers of buoyancy and gravity varies from individual to individual and depends on factors such as age, gender, and body composition.^{16, 23, 36, 37)} Usually, the distance is

greater for males than for females¹⁹⁾ and adults compared with children.^{21, 38)} In studies on body composition, the density of the fat component is assumed to be approximately 0.9007 g/cm^3 and that of fat-free muscle is approximately 1.066 g/cm^3 .³⁹⁾ Because water density is 1.00 g/cm^3 , fat will float and muscle will sink. The distance between the centers of buoyancy and gravity decreases when the fat component is concentrated in the lower body.²²⁾ The use of buoyancy tools such as pull buoys (which are widely used as swimming tools around the world) also affects underwater torque. Swimmers place the pull buoy between their thighs or their ankles while swimming, and the pull buoy reduces underwater torque by providing improved flotation support for the hips and legs.²²⁾ However, in competitions, swimmers are not allowed to use support tools. It is impossible to change the age of a swimmer and impractical to alter gender, and body composition cannot be changed within a short period of time. Hence, it is imperative that swimmers find other techniques to reduce underwater torque.

Swimmer's drag and BSA

Underwater torque increases the frontal surface area, resulting in an increase in swimmer's drag. In addition to the increasing frontal surface area due to underwater torque, the BSA is an important factor that affects a swimmer's drag.³⁾

⁴⁾ Frictional drag, which is one type of swimmers' drag, can be calculated from the density of the water, gliding velocity, and BSA by numerical simulations (computer fluid dynamics).^{5, 15)} The BSA was calculated using the formulas developed by Du Bois³⁰⁾ based on height and weight. In our study, we found no significant difference in the BSA between participants in the high-performance group and those in the low-performance group.

Abdominal drawing-in maneuver

In our study, we noted an increased thickness of the anterolateral abdominal wall and a decrease in CSA at the umbilical level in the streamlined body position. This action is similar to the abdominal drawing-in maneuver (ADIM), a body trunk exercise. The ADIM is a method to increase abdominal pressure by pulling the abdominal walls to the inside, so that the TrA and oblique abdominal muscles are contracted.⁴⁰⁾ Because the stability of the lumbar trunk is effectively accomplished through the increase in abdominal pressure, the ADIM has been reported to be important in rehabilitation of lower back pain.^{41, 42)} Previous researchers have studied the action of the abdominal wall muscles during ADIM using ultrasound imaging, MRI, and electromyography.^{43, 44)} The muscle bellies of the anterolateral abdominal wall were observed to thicken and shorten in length

during the ADIM, whereas the RA muscle did not thicken during the ADIM.^{43, 45)}

We also observed these muscle-thickening responses in our study. The thickness of the anterolateral abdominal wall muscle increased significantly from the resting position to the streamlined body position, whereas the thickness of the RA muscle did undergo a significant change. A prior study also reported that the CSA of the trunk (including the abdominal cavity and trunk muscles, but excluding the subcutaneous tissue) at the L3–L4 disc decreased with the ADIM.^{41, 43)} This CSA differed from our study in terms of measurement range and measurement height; however, we also observed a decrease in the CSA at the umbilical level in our study. Thus, despite being instructed to hold only the streamlined position, it seems that these participants also unconsciously made similar movements to the ADIM. Because abdominal contraction, similar to ADIM, occurred unconsciously, it was impossible to assess the gliding distance both with and without abdominal contraction.

Abdominal core muscles

The abdominal muscles support the trunk, allow movement, and hold organs in place by regulating internal abdominal pressure. The core musculature includes both the deep and superficial muscles of the lumbopelvic-hip complex. The

constituent muscles are the IO, transversus abdominis, transverse spinal column, quadratus lumborum, psoas major and minor, RA, EO, erector spinae, vastus lateralis, gluteus medius and medius, hamstrings, and rectus femoris ⁴⁶⁻⁵²).

Strengthening the core muscles can reduce the risk of lower extremity injuries and improve performance ^{53, 54}).

Moreover, core muscle strengthening can decrease the risk of lumbar spine injury by increasing spinal stability ⁴⁶).

Core muscle recruitment

Several studies have investigated the recruitment of the trunk muscles during various exercises. In the side bridge exercise, the ball exercise resulted in greater activity of the IO muscles than a bench with a stable surface ⁵⁵). The side bridge exercise produces greater RA, EO, and IO muscle activities than the crunch exercise ⁵⁶). Significantly greater activity of the EO abdominal muscles and lumbar paraspinal column was observed in the side bridge exercise in comparison with the prone bridge exercise ⁵⁷). The crunch exercise is effective in activating the IO and transverse abdominal muscles, whereas the side bridge exercise is effective in activating the quadratus lumborum muscle ^{58, 59}).

Differences between land and water

Water is different from land in many ways because of the buoyancy that occurs in water. Underwater exercise is sometimes performed in the hope that buoyancy will reduce the water load. The apparent body weight in water is defined as the gravity force minus the buoyancy force. Body weight decreases to approximately 30% in chest-high water ⁶⁰. In the present study, the abdominal core muscles caused the cranial movement of the abdominal organs. Because the abdominal core muscles are located in the front of the body, the effort to pull up the heavy internal organs in a prone posture is significant. Therefore, it is considered more difficult to move on land than in water.

Gliding distance and kick force

Several studies have examined the relationship between gliding distance and kick-start ⁶¹. If possible, it would be desirable to maintain a constant force to kick the wall. However, a device to eject swimmers with a constant force would be extremely large. For this reason, in the previous studies, the subjects were asked to perform their maximal push-off from the wall ⁶². Similarly in our study, the subjects were instructed to kick the wall with maximum force. To ensure uniformity of the data, five measurements were obtained, and the average value

was used.

Future prospects

The reason for the difference in CSA between the high- and low-performance groups has not been clarified. The thickness of the RA and lateral abdominal muscles was similar in both the high- and low-performance groups. The longer the YSP, the longer the gliding distance; therefore, the technique may play a role. This issue needs to be investigated in the future.

Limitations

This study has several limitations. First, the streamlined body position on MRI may not be exactly the same as the streamlined body position in water. However, obtaining MR images in water it is impossible because of the interference caused by the water. To ameliorate this, we used a soft cushion on the ventral side so that participants could hold the streamlined body position easily and checked the body position through the monitor during MRI scans. Second, swimmers do not hold their breath while swimming but rather breathe out normally under water. This differs from the glide phase performed in our study. We measured the maximum gliding distance while the participants held their breath while gliding. Thus, our

study results based on this glide may not be completely applicable to normal swimming. Third, although gliding distance is primarily influenced by drag, other factors such as physique, push-off characteristics, and swimsuits may have an effect.⁶³⁻⁶⁵⁾ In this sense, some precaution should be taken when interpreting the gliding performance in our study, as it might have some biases.⁶²⁾ Our participants were college swimmers, so they were not beginners, and they had a certain amount of swimming ability. There was no physical difference between the two groups. All participants wore standard swimsuits, rather than high-performance swimsuits. Thus, we assumed that these factors are comparable between the two groups in this study. Fourth, the center of buoyancy position was not measured. Even if the center of gravity moves to the cranial side, the distance between the centers of buoyancy and gravity does not shrink if the buoyancy also moves to the head side. Because the lung position is anatomically stable, we assumed that the buoyancy was in the same position.

VII. CONCLUSION

As compared with the low-performance group, swimmers with high gliding performance exhibit different abdominal cavity shapes in the streamlined body position, which causes cranial movement of the abdominal organs. This movement can reduce underwater torque, prevent the legs from sinking during swimming, and have a positive effect on gliding performance.

VIII. REFERENCES

1. Chatard JC, Lavoie JM, Bourgoïn B, et al. The contribution of passive drag as a determinant of swimming performance. *International journal of sports medicine*. 1990;11(5):367-72.
2. Vilas-Boas JP, Costa L, Fernandes RJ, et al. Determination of the drag coefficient during the first and second gliding positions of the breaststroke underwater stroke. *Journal of applied biomechanics*. 2010;26(3):324-31.
3. Zamparo P, Gatta G, Pendergast D, et al. Active and passive drag: the role of trunk incline. *European journal of applied physiology*. 2009;106(2):195-205.
4. Barbosa TM, Yam JW, Lum D, et al. Arm-pull thrust in human swimming and the effect of post-activation potentiation. *Scientific reports*. 2020;10(1):8464.
5. Barbosa TM, Ramos R, Silva AJ, et al. Assessment of passive drag in swimming by numerical simulation and analytical procedure. *Journal of sports sciences*. 2018;36(5):492-8.
6. Naemi R, Easson WJ, Sanders RH. Hydrodynamic glide efficiency in swimming. *Journal of science and medicine in sport*. 2010;13(4):444-51.
7. Vantorre J, Chollet D, Seifert L. Biomechanical analysis of the swim-start: a review. *Journal of sports science & medicine*. 2014;13(2):223-31.
8. Starling RD, Costill DL, Trappe TA, et al. Effect of swimming suit design on the energy demands of swimming. *Medicine and science in sports and exercise*. 1995;27(7):1086-9.

9. Scurati R, Gatta G, Michielon G, et al. Techniques and considerations for monitoring swimmers' passive drag. *Journal of sports sciences*. 2019;37(10):1168-80.
10. Yuan ZM, Li M, Ji CY, et al. Steady hydrodynamic interaction between human swimmers. *Journal of the Royal Society, Interface*. 2019;16(150):20180768.
11. Novais ML, Silva AJ, Mantha VR, et al. The Effect of Depth on Drag During the Streamlined Glide: A Three-Dimensional CFD Analysis. *Journal of human kinetics*. 2012;33:55-62.
12. Cortesi M, Gatta G. Effect of The Swimmer's Head Position on Passive Drag. *Journal of human kinetics*. 2015;49:37-45.
13. Cortesi M, Gatta G, Michielon G, et al. Passive Drag in Young Swimmers: Effects of Body Composition, Morphology and Gliding Position. *International journal of environmental research and public health*. 2020;17(6).
14. Payton C, Hogarth L, Burkett B, et al. Active Drag as a Criterion for Evidence-based Classification in Para Swimming. *Medicine and science in sports and exercise*. 2020;52(7):1576-84.
15. Barbosa TM, Morais JE, Forte P, et al. A Comparison of Experimental and Analytical Procedures to Measure Passive Drag in Human Swimming. *PloS one*. 2015;10(7):e0130868.
16. Zamparo P, Antonutto G, Capelli C, et al. Effects of body size, body density, gender and growth on underwater torque. *Scandinavian journal of medicine & science in sports*. 1996;6(5):273-80.
17. Kjendlie PL, Stallman RK, Stray-Gundersen J. Passive and active floating torque during swimming. *European journal of applied physiology*. 2004;93(1-2):75-81.

18. Yanai T. Rotational effect of buoyancy in frontcrawl: Does it really cause the legs to sink? *Journal of biomechanics*. 2001;34(2):235-43.
19. McLean SP, Hinrichs RN. Sex differences in the centre of buoyancy location of competitive swimmers. *Journal of sports sciences*. 1998;16(4):373-83.
20. Gagnon M, Montpetit R. Technological development for the measurement of the center of volume in the human body. *Journal of biomechanics*. 1981;14(4):235-41.
21. Zamparo P, Capelli C, Termin B, et al. Effect of the underwater torque on the energy cost, drag and efficiency of front crawl swimming. *European journal of applied physiology and occupational physiology*. 1996;73(3-4):195-201.
22. Cortesi M, Fantozzi S, Di Michele R, et al. Passive drag reduction using full-body swimsuits: the role of body position. *Journal of strength and conditioning research*. 2014;28(11):3164-71.
23. Zamparo P, Lazzer S, Antoniazzi C, et al. The interplay between propelling efficiency, hydrodynamic position and energy cost of front crawl in 8 to 19-year-old swimmers. *European journal of applied physiology*. 2008;104(4):689-99.
24. Molina DK, DiMaio VJ. Normal organ weights in men: part II-the brain, lungs, liver, spleen, and kidneys. *The American journal of forensic medicine and pathology*. 2012;33(4):368-72.
25. Protection ICoR. Adult reference computational phantoms. Elsevier ICRP Publication 110. 2009;39(2).
26. Hayes AR, Gayzik FS, Moreno DP, et al. Abdominal Organ Location, Morphology, and Rib

Coverage for the 5(th), 50(th), and 95(th) Percentile Males and Females in the Supine and Seated Posture using Multi-Modality Imaging. Annals of advances in automotive medicine Association for the Advancement of Automotive Medicine Annual Scientific Conference. 2013;57:111-22.

27. Hayes AR, Gayzik FS, Moreno DP, et al. Comparison of organ location, morphology, and rib coverage of a midsized male in the supine and seated positions. Computational and mathematical methods in medicine. 2013;2013:419821.

28. Deukmedjian AR, Le TV, Dakwar E, et al. Movement of abdominal structures on magnetic resonance imaging during positioning changes related to lateral lumbar spine surgery: a morphometric study: Clinical article. Journal of neurosurgery Spine. 2012;16(6):615-23.

29. Howes MK, Hardy WN, Beillas P. The effects of cadaver orientation on the relative position of the abdominal organs. Annals of advances in automotive medicine Association for the Advancement of Automotive Medicine Annual Scientific Conference. 2013;57:209-24.

30. Du Bois D, Du Bois EF. A formula to estimate the approximate surface area if height and weight be known. 1916. Nutrition (Burbank, Los Angeles County, Calif). 1989;5(5):303-11; discussion 12-3.

31. Hochstein S, Baumgart M, Müller R, et al. Determine the Center of Mass Position in Human Undulatory Swimming: A Static Approach. International journal of sports science and physical education. 2016;Volume 1(Issue 2):21-7.

32. Watanabe Y, Wakayoshi K, Nomura T. New evaluation index for the retainability of a

swimmer's horizontal posture. PloS one. 2017;12(5):e0177368.

33. Sekiguchi Y, Owaki D, Honda K, et al. Ankle-foot orthosis with dorsiflexion resistance using spring-cam mechanism increases knee flexion in the swing phase during walking in stroke patients with hemiplegia. Gait & posture. 2020;81:27-32.

34. Kanda Y. Investigation of the freely available easy-to-use software 'EZR' for medical statistics. Bone Marrow Transplant. 2013;48(3):452-8.

35. Capelli C, Zamparo P, Cigalotto A, et al. Bioenergetics and biomechanics of front crawl swimming. Journal of applied physiology (Bethesda, Md : 1985). 1995;78(2):674-9.

36. Zamparo P, Capelli C, Pendergast D. Energetics of swimming: a historical perspective. European journal of applied physiology. 2011;111(3):367-78.

37. Dopsaj M, Zuoziene IJ, Milić R, et al. Body Composition in International Sprint Swimmers: Are There Any Relations with Performance? International journal of environmental research and public health. 2020;17(24).

38. Kjendlie PL, Ingjer F, Stallman RK, et al. Factors affecting swimming economy in children and adults. European journal of applied physiology. 2004;93(1-2):65-74.

39. Prior BM, Modlesky CM, Evans EM, et al. Muscularity and the density of the fat-free mass in athletes. Journal of applied physiology (Bethesda, Md : 1985). 2001;90(4):1523-31.

40. Park SD, Yu SH. The effects of abdominal draw-in maneuver and core exercise on abdominal muscle thickness and Oswestry disability index in subjects with chronic low back pain. Journal of

exercise rehabilitation. 2013;9(2):286-91.

41. Hides J, Wilson S, Stanton W, et al. An MRI investigation into the function of the transversus abdominis muscle during "drawing-in" of the abdominal wall. *Spine*. 2006;31(6):E175-8.

42. Kaping K, Ang BO, Rasmussen-Barr E. The abdominal drawing-in manoeuvre for detecting activity in the deep abdominal muscles: is this clinical tool reliable and valid? *BMJ open*. 2015;5(12):e008711.

43. Hides JA, Boughen CL, Stanton WR, et al. A magnetic resonance imaging investigation of the transversus abdominis muscle during drawing-in of the abdominal wall in elite Australian Football League players with and without low back pain. *The Journal of orthopaedic and sports physical therapy*. 2010;40(1):4-10.

44. Chon SC, Chang KY, You JS. Effect of the abdominal draw-in manoeuvre in combination with ankle dorsiflexion in strengthening the transverse abdominal muscle in healthy young adults: a preliminary, randomised, controlled study. *Physiotherapy*. 2010;96(2):130-6.

45. Badiuk BW, Andersen JT, McGill SM. Exercises to activate the deeper abdominal wall muscles: the Lewit: a preliminary study. *Journal of strength and conditioning research*. 2014;28(3):856-60.

46. Axler CT, McGill SM. Low back loads over a variety of abdominal exercises: searching for the safest abdominal challenge. *Medicine and science in sports and exercise*. 1997;29(6):804-11.

47. Escamilla RF, Babb E, DeWitt R, et al. Electromyographic analysis of traditional and

nontraditional abdominal exercises: implications for rehabilitation and training. *Physical therapy*. 2006;86(5):656-71.

48. Escamilla RF, McTaggart MS, Fricklas EJ, et al. An electromyographic analysis of commercial and common abdominal exercises: implications for rehabilitation and training. *The Journal of orthopaedic and sports physical therapy*. 2006;36(2):45-57.

49. McGill S, Juker D, Kropf P. Appropriately placed surface EMG electrodes reflect deep muscle activity (psoas, quadratus lumborum, abdominal wall) in the lumbar spine. *Journal of biomechanics*. 1996;29(11):1503-7.

50. McGill SM. Distribution of tissue loads in the low back during a variety of daily and rehabilitation tasks. *Journal of rehabilitation research and development*. 1997;34(4):448-58.

51. Sternlicht E, Rugg S, Fujii LL, et al. Electromyographic comparison of a stability ball crunch with a traditional crunch. *Journal of strength and conditioning research*. 2007;21(2):506-9.

52. Vera-Garcia FJ, Grenier SG, McGill SM. Abdominal muscle response during curl-ups on both stable and labile surfaces. *Physical therapy*. 2000;80(6):564-9.

53. Hewett TE, Lindenfeld TN, Riccobene JV, et al. The effect of neuromuscular training on the incidence of knee injury in female athletes. A prospective study. *The American journal of sports medicine*. 1999;27(6):699-706.

54. Myer GD, Chu DA, Brent JL, et al. Trunk and hip control neuromuscular training for the prevention of knee joint injury. *Clinics in sports medicine*. 2008;27(3):425-48, ix.

55. Behm DG, Leonard AM, Young WB, et al. Trunk muscle electromyographic activity with unstable and unilateral exercises. *Journal of strength and conditioning research*. 2005;19(1):193-201.
56. Kavcic N, Grenier S, McGill SM. Quantifying tissue loads and spine stability while performing commonly prescribed low back stabilization exercises. *Spine*. 2004;29(20):2319-29.
57. Ekstrom RA, Donatelli RA, Carp KC. Electromyographic analysis of core trunk, hip, and thigh muscles during 9 rehabilitation exercises. *The Journal of orthopaedic and sports physical therapy*. 2007;37(12):754-62.
58. Teyhen DS, Rieger JL, Westrick RB, et al. Changes in deep abdominal muscle thickness during common trunk-strengthening exercises using ultrasound imaging. *The Journal of orthopaedic and sports physical therapy*. 2008;38(10):596-605.
59. McGill S, Juker D, Kropf P. Quantitative intramuscular myoelectric activity of quadratus lumborum during a wide variety of tasks. *Clinical biomechanics (Bristol, Avon)*. 1996;11(3):170-2.
60. Orselli MI, Duarte M. Joint forces and torques when walking in shallow water. *Journal of biomechanics*. 2011;44(6):1170-5.
61. Matúš I, Ružbarský P, Vadašová B. Key Parameters Affecting Kick Start Performance in Competitive Swimming. *International journal of environmental research and public health*. 2021;18(22).
62. Barbosa TM, Costa MJ, Morais JE, et al. How Informative are the Vertical Buoyancy and the Prone Gliding Tests to Assess Young Swimmers' Hydrostatic and Hydrodynamic Profiles? *Journal of*

human kinetics. 2012;32:21-32.

63. Chatard JC, Wilson B. Effect of fastskin suits on performance, drag, and energy cost of swimming. *Medicine and science in sports and exercise*. 2008;40(6):1149-54.

64. Mollendorf JC, Termin AC, 2nd, Oppenheim E, et al. Effect of swim suit design on passive drag. *Medicine and science in sports and exercise*. 2004;36(6):1029-35.

65. Roberts BS, Kamel KS, Hedrick CE, et al. Effect of a FastSkin suit on submaximal freestyle swimming. *Medicine and science in sports and exercise*. 2003;35(3):519-24.

IX. ACKNOWLEDGEMENTS

I wish to thank Professor Masahiro Kohzuki, Shin-Ichi Izumi, and Kei Takase for providing valuable advices regarding this study. I would like to thank Dr. Hideki Ota, Satoshi Higuchi, Yusuke Sekiguchi, Takaaki Kakihana, Haruka Sato, and Tomoyoshi Kimura for their help with the experiments. This work was supported by the Advanced Graduate Program for Future Medicine and Health Care, Tohoku University.

X. FIGURES

Figure 1

Schematic of the streamlined body position in water. The white circle indicates the center of buoyancy, and the black circle indicates the center of gravity. The white arrow indicates buoyancy force, and the black arrows indicate gravity force. Because the lungs have a lower density and are located in the chest, the center of buoyancy is always on the cranial side, and the center of gravity is always on the caudal side. An object rotates in water until the center of buoyancy and the center of gravity are aligned vertically. As shown, sinking legs led to increased frontal surface area. This is disadvantageous to swimming performance.

Figure 2

The photos show a swimmer floating his legs in the streamlined body position by merely drawing in his abdominal muscles. He raises his hands, but his lower body sinks (a). After that, his legs float without the use of any tools, propulsion, or any other remarkable action such as underwater kicking (b). The drawing-in belly maneuver causes cranial movement of the abdominal organs and reduces the distance between the centers of buoyancy and gravity, reducing underwater

torque.

Figure 3

CT images showing resting position (a), streamlined body position (b), and superimposed on each other (c). The results of these images demonstrated that there was a migration of approximately two vertebral body distances to the head side in the liver, kidney, and spleen in the streamlined position.

Figure 4

Images showing a lateral view of the lung in the streamlined position (a), lateral view in the resting position (b), superimposed on the lateral view (c), and the frontal view (d). In the sagittal view at the left kidney level, the maximum value of the anteroposterior system of the lung was defined as the anteroposterior diameter. In the coronal view at the tracheal bifurcation, the vertical diameter was defined as the distance from the tracheal bifurcation to the left lung base. The anteroposterior diameter of the lung increased from 156 mm to 166 mm, and the vertical diameter decreased from 217 mm to 151 mm.

Figure 5

Sagittal view images showing the spines in the resting position (a) and streamlined position (b). The angle between the inferior border of the Th12 vertebra and the superior border of the S1 vertebra was measured. The lumbar lordosis decreased from 81° to 40°.

Figure 6

Images showing the axial image at the umbilicus level in the resting position (a) and streamlined position (b). The lateral abdominal wall muscles (transversus abdominis, external oblique, and internal oblique) increased from 17 mm to 31 mm.

Figure 7

The gliding distance in the streamlined body position was measured for each participant in an indoor pool, as shown. The gliding distance was defined as the maximum distance the swimmer could cover in the streamlined body position without performing any arm strokes or kicks. The pool was 25-m long and had a depth of 1.3 m. Participants used standard swimsuits. They began by standing on the pool floor, then submerged and maximally pushed off the wall in the streamlined body position.

Figure 8

MR examinations were performed using a 3.0-T whole-body MR scanner. Participants were placed in the prone position with their hands up and overlapping, head between the extended arms, and feet together and plantar flexed.

Figure 9

Axial MR image at the upper liver level showing measurements of the cross-sectional area (a). Axial MR image at the lower lung level showing measurements of the cross-sectional area (b). Axial MR image at the umbilical level showing measurements of the cross-sectional area and thickness of the abdominal muscles (c). Sagittal MR image at the left kidney level showing the abdominal cavity, which is marked in yellow (d). (a) Upper liver level. (b) Lower lung level. (c) Umbilical level.

Figure 10

Participants were placed on the balance board in the supine position, and measurements were performed in both the streamlined body position and resting

position. For the streamlined body position, participants were instructed to hold a streamlined position as if underwater. For the resting position, participants were instructed to raise their arms above their head, as in the streamlined body position, and to relax their body.

Figure 11

Schematic of the reaction board method used for measuring the center of gravity. The black circle indicates the center of gravity, and the black rectangle indicates the force plate. CG is the distance from the feet to the participant's center of gravity, and L is the length between the tip of the longest finger and the soles of the feet. The measurement point was at the tip of the finger, whereas the pivot point was at the soles of the feet. We used the force plate to measure the reaction force at the tip of the finger (without the weight of the balance board itself).

Figure 12

Box plot of the changes in CSA between the high-performance and low-performance groups at the upper liver level. The box plots show the median (center line), interquartile range (hinges), and 10th and 90th percentiles (whiskers). In the high-performance group, the change in the CSA from resting to

streamlined body positions was 36.8 cm² (median, interquartile range: 28.7–67.3).

In the low-performance group, the change in the CSA from resting to streamlined body positions was 16.4 cm² (9.3–22.2). The changes in the CSA were significantly greater in the high-performance group than in the low-performance group at the upper liver level (Mann–Whitney *U* test, *P* = 0.036).

Figure 13

Box plot of the changes in the CSA between the high-performance and low-performance groups at the lower lung level. The box plots show the median (center line), interquartile range (hinges), and 10th and 90th percentiles (whiskers). In the high-performance group, the change in the CSA from the resting to streamlined body positions was 23.2 cm² (median, interquartile range: 17.3–44.2). In the low-performance group, the change in the CSA from the resting to the streamlined body positions was –5.1 cm² (–15.4 to 11.6). The change in the CSA was significantly greater in the high-performance group than in the low-performance group at the lower lung level (Mann–Whitney *U* test, *P* < 0.01).

Figure. 14

Box plot of the changes in CSA between the high-performance and

low-performance groups at the umbilical level. The box plots show the median (center line), interquartile range (hinges), and 10th and 90th percentiles (whiskers). In the high-performance group, the change in CSA from the resting to the streamlined body positions was -37.4 cm^2 (median, interquartile range: -47.4 to -24.9). In the low-performance group, the change in the CSA from the resting to the streamlined body positions was -1.2 cm^2 (-18.1 to 0.75). The change in the CSA was significantly greater in the high-performance group than in the low-performance group at the umbilical level (Mann–Whitney U test, $P < 0.01$).

Figure 15

Relationship between gliding distance and years of swimming practice (YSP). Spearman's correlation between gliding distance and YSP is 0.74.

Figure 16

Relationship between gliding distance and changes in CSA at the upper liver level. Spearman's correlation between gliding distance and CSA at the upper liver level is 0.63.

Figure 17

Relationship between gliding distance and changes in CSA at the lower lung level.

Spearman's correlation between gliding distance and CSA at the lower lung level is 0.78.

Figure 18

Relationship between gliding distance and changes in CSA at the umbilical level.

Spearman's correlation between gliding distance and CSA at the umbilical level is -0.78.

Figure 19

Relationship between gliding distance and the ratio of CSA at the upper liver level to umbilical level (resting position). Spearman's correlation between gliding distance and the ratio of CSA at the upper liver level to umbilical level (resting position) is 0.072.

Figure 20

Relationship between gliding distance and the ratio of CSA at the upper liver level to umbilical level (streamlined body position). Spearman's correlation between gliding distance and the ratio of CSA at the upper liver level to umbilical level

(streamlined body position) is 0.78.

Figure 21

Relationship between gliding distance and the ratio of CSA at the lower lung level to umbilical level (resting position). Spearman's correlation between gliding distance and the ratio of CSA at the lower lung level to umbilical level (resting position) is -0.16.

Figure 22

Relationship between gliding distance and the ratio of CSA at the lower lung level to umbilical level (streamlined body position). Spearman's correlation between gliding distance and the ratio of CSA at the lower lung level to umbilical level (streamlined body position) is 0.76.

Figure 23

Sagittal MR images at the left kidney level show the abdominal cavity, which is marked in yellow. (1) Upper liver level. (2) Lower lung level. (3) Umbilical level. A, A': Case 1 is a representative case of the high-performance group: the years of swimming practice (YSP) was 8 years, and the gliding distance was 13 m. From

the resting position (A) to the streamlined body position (A'). B, B': Case 2 is a representative case of the low-performance group: YSP was 1 year, and gliding distance was 8 m. From the resting position (B) to the streamlined body position (B'). The CSA in the high-performance group (as shown in case 1: A, A') increased at the upper liver and lower lung levels and decreased at the umbilical level in the streamlined body position. These changes in CSA were significantly greater than those of the low-performance group at all three levels (Figures 12, 13, and 14). This change in abdominal cavity shape may cause cranial-side movement of the abdominal organs.

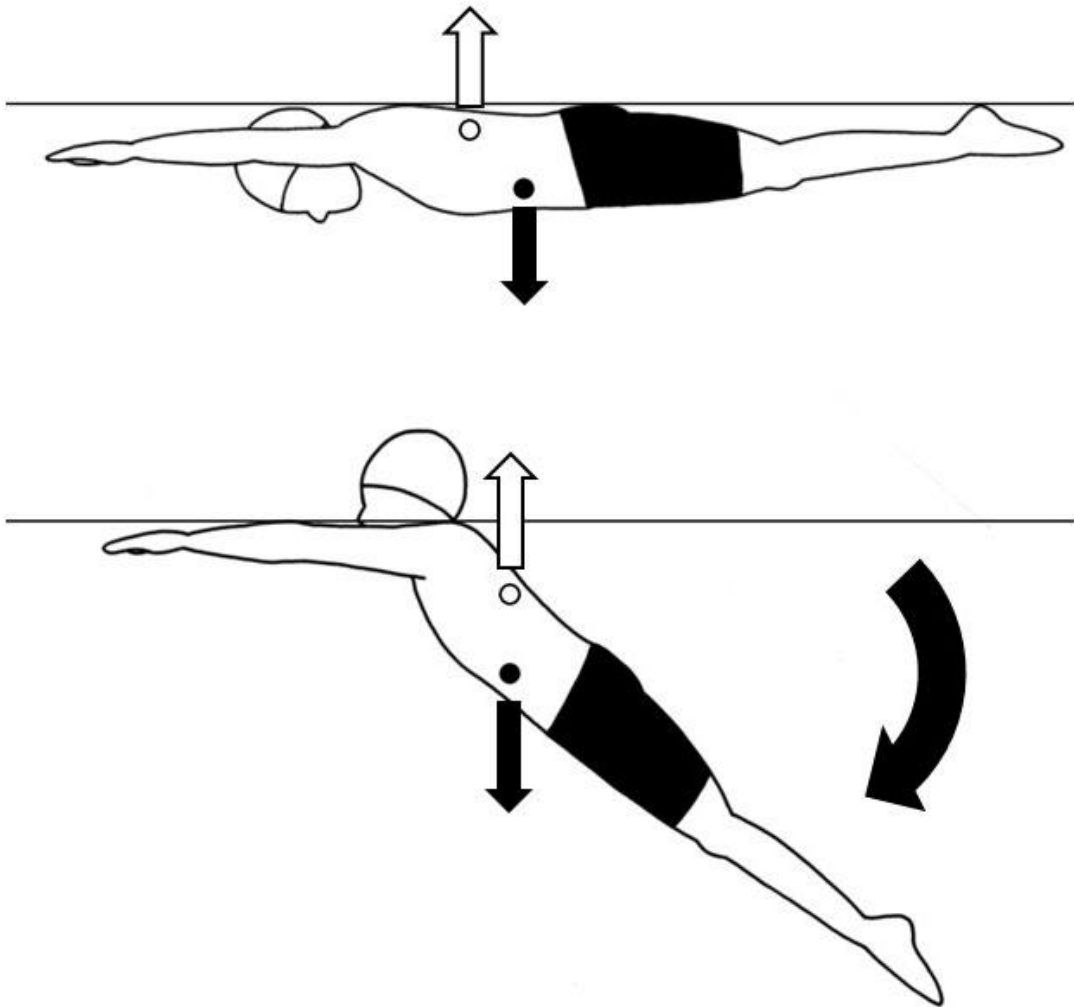


Figure 1



Figure 2

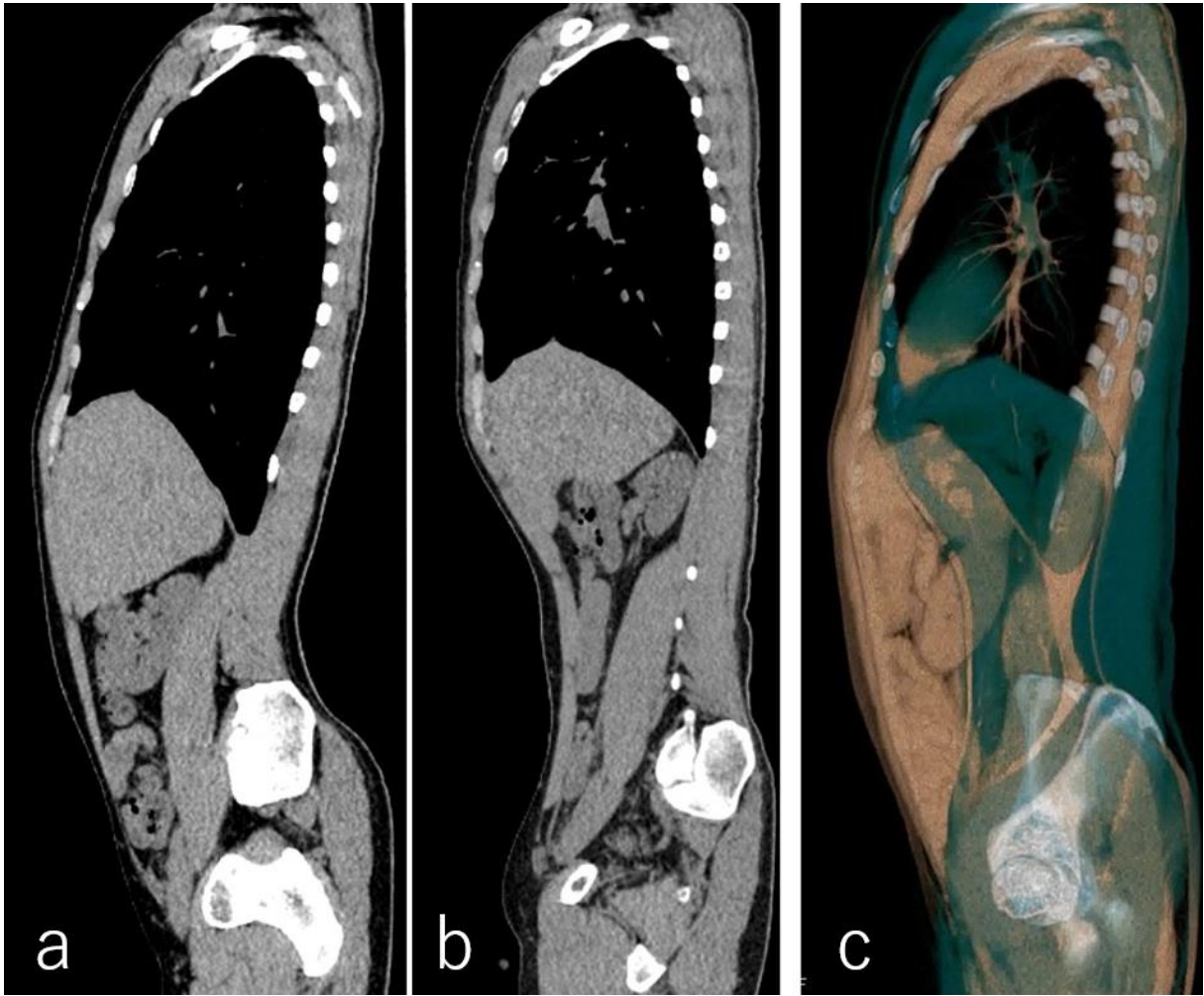


Figure 3

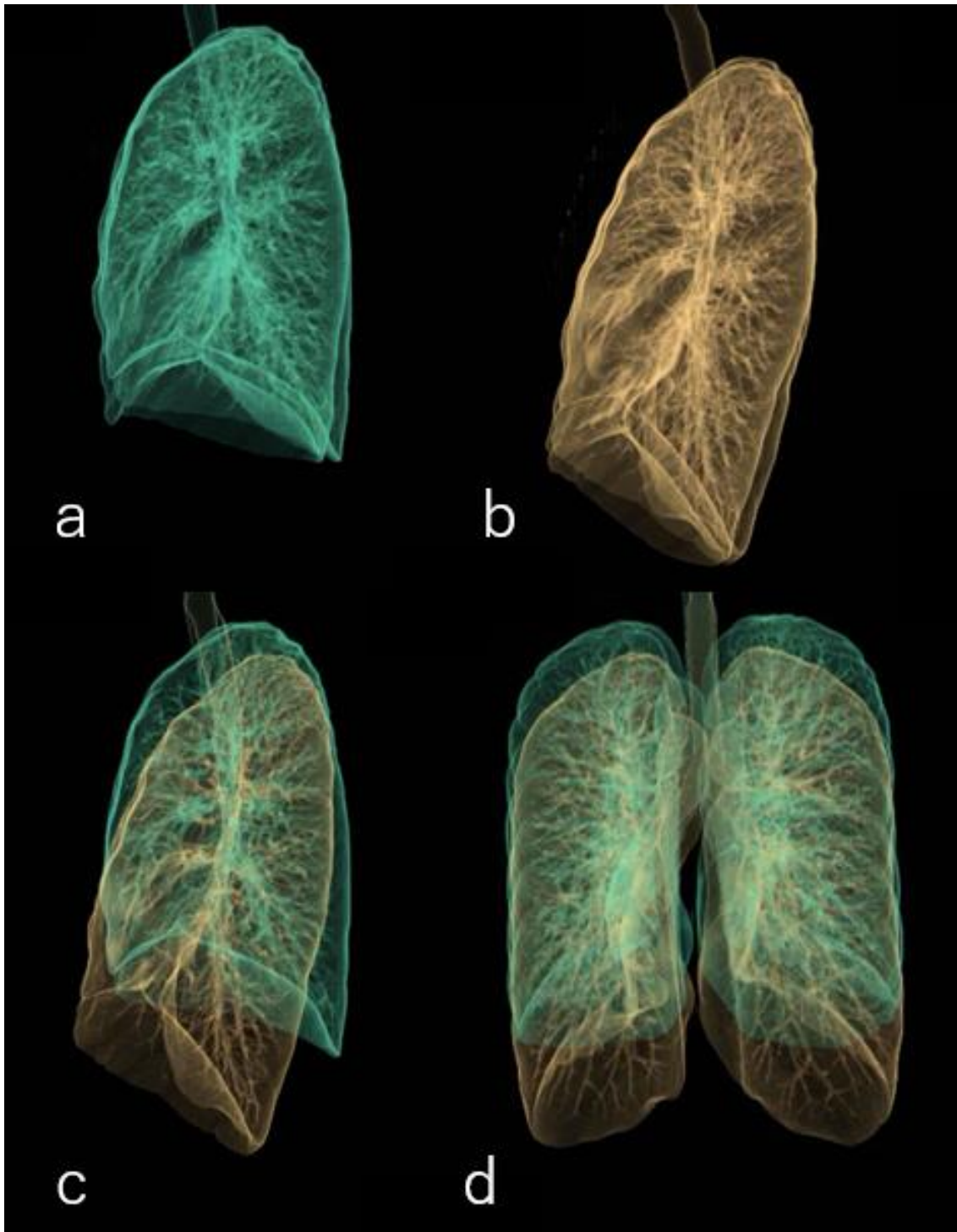


Figure 4

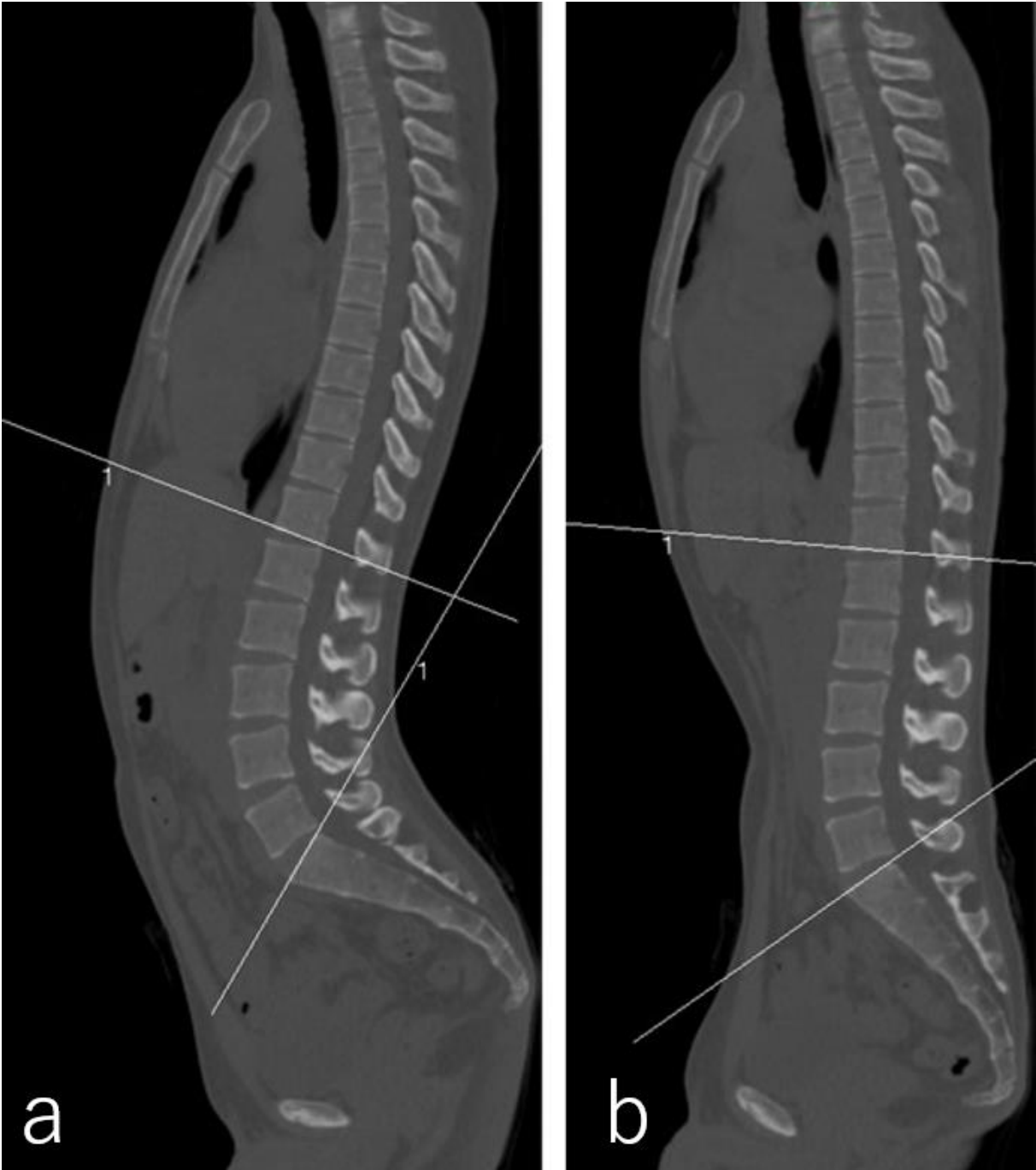


Figure 5

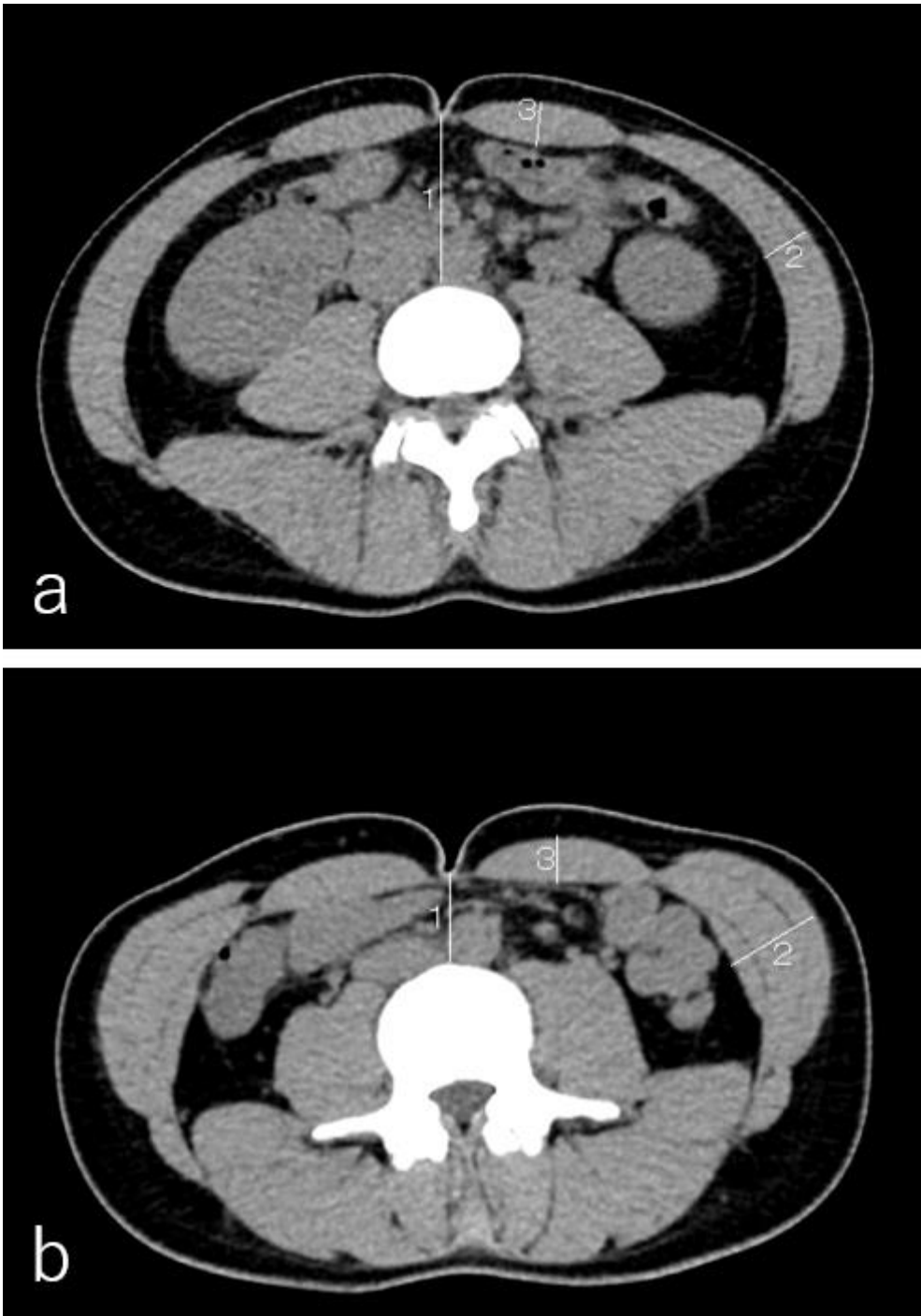


Figure 6

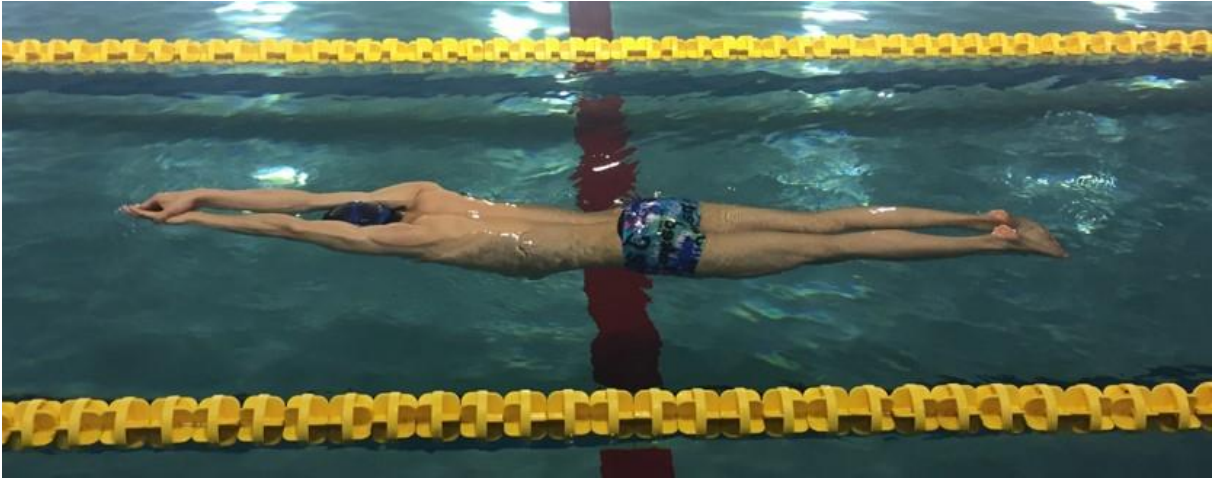


Figure 7



Figure 8

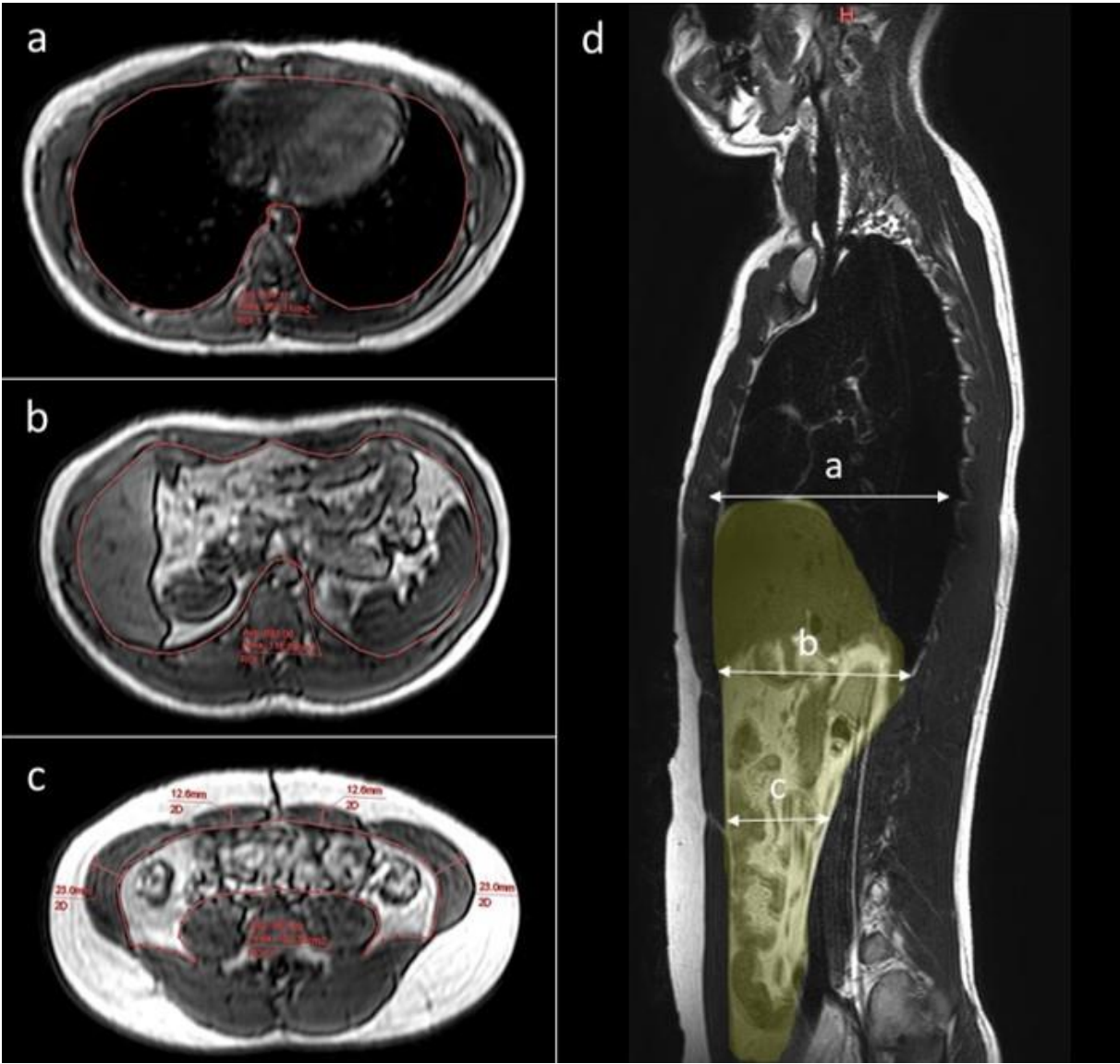


Figure 9



Figure 10

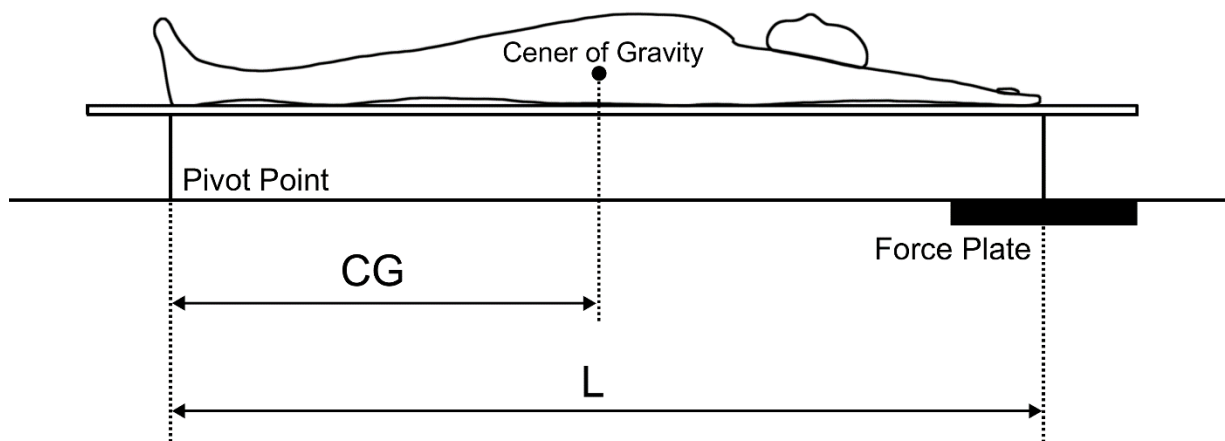


Figure 11

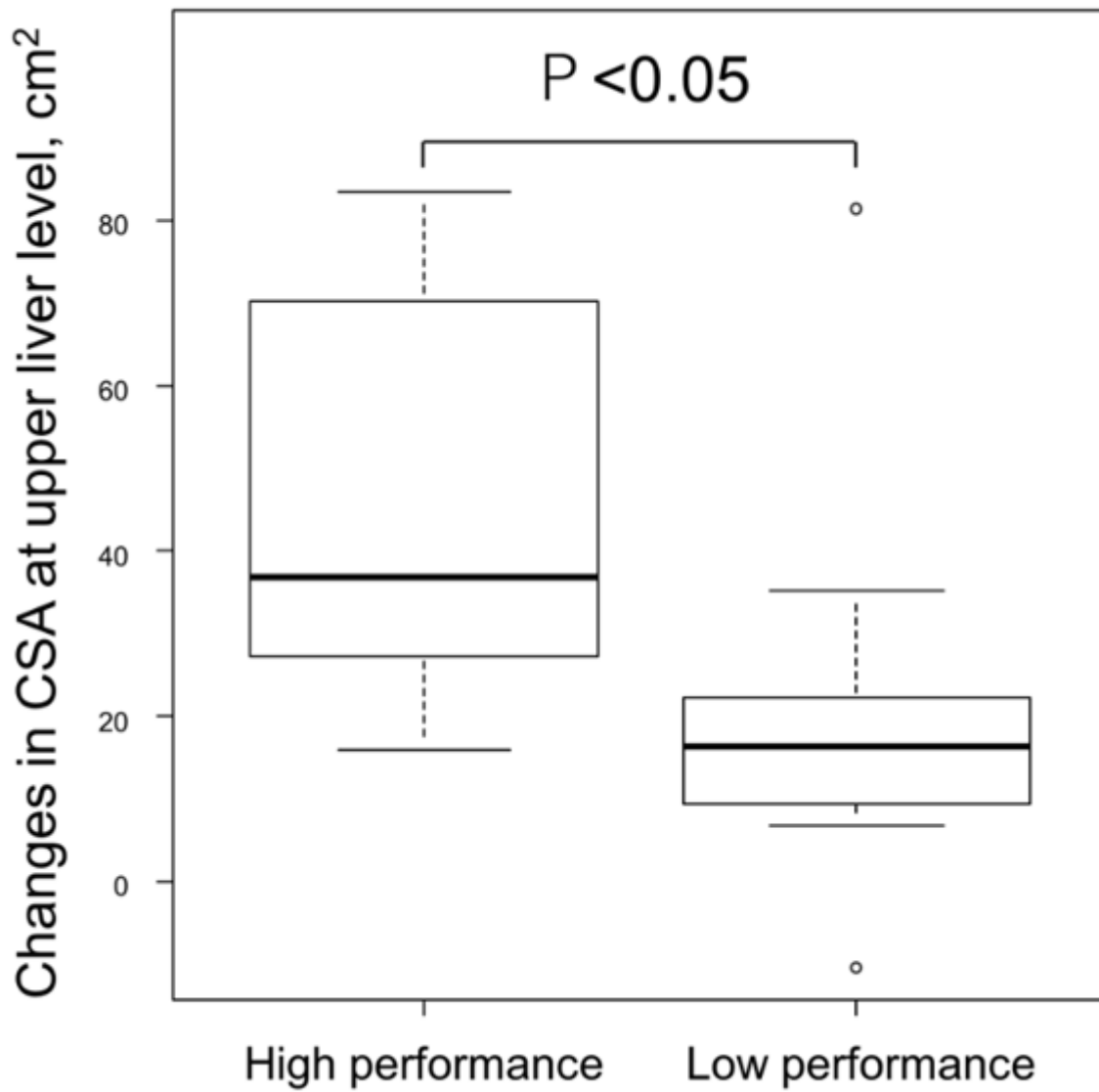


Figure 12

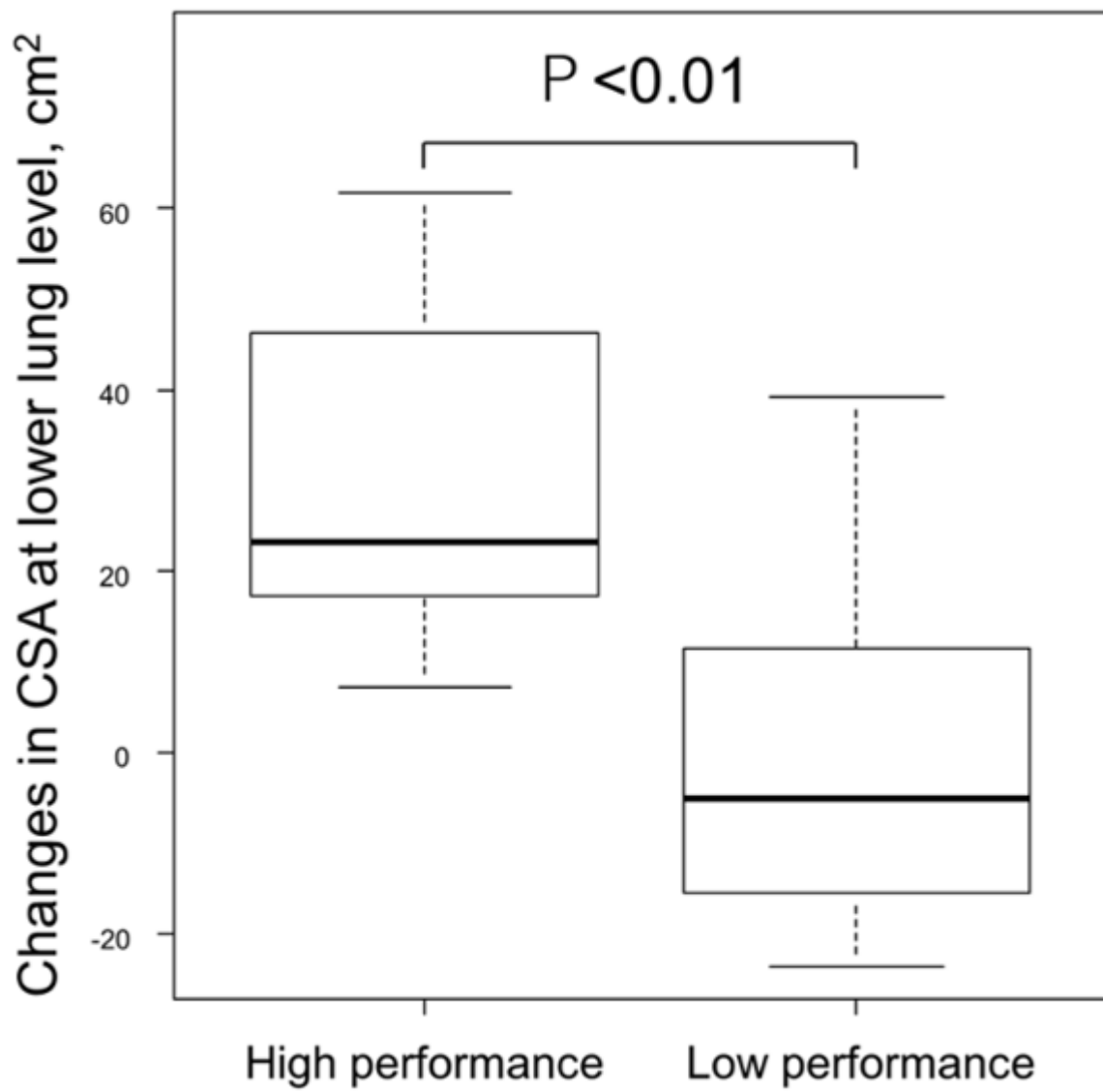


Figure 13

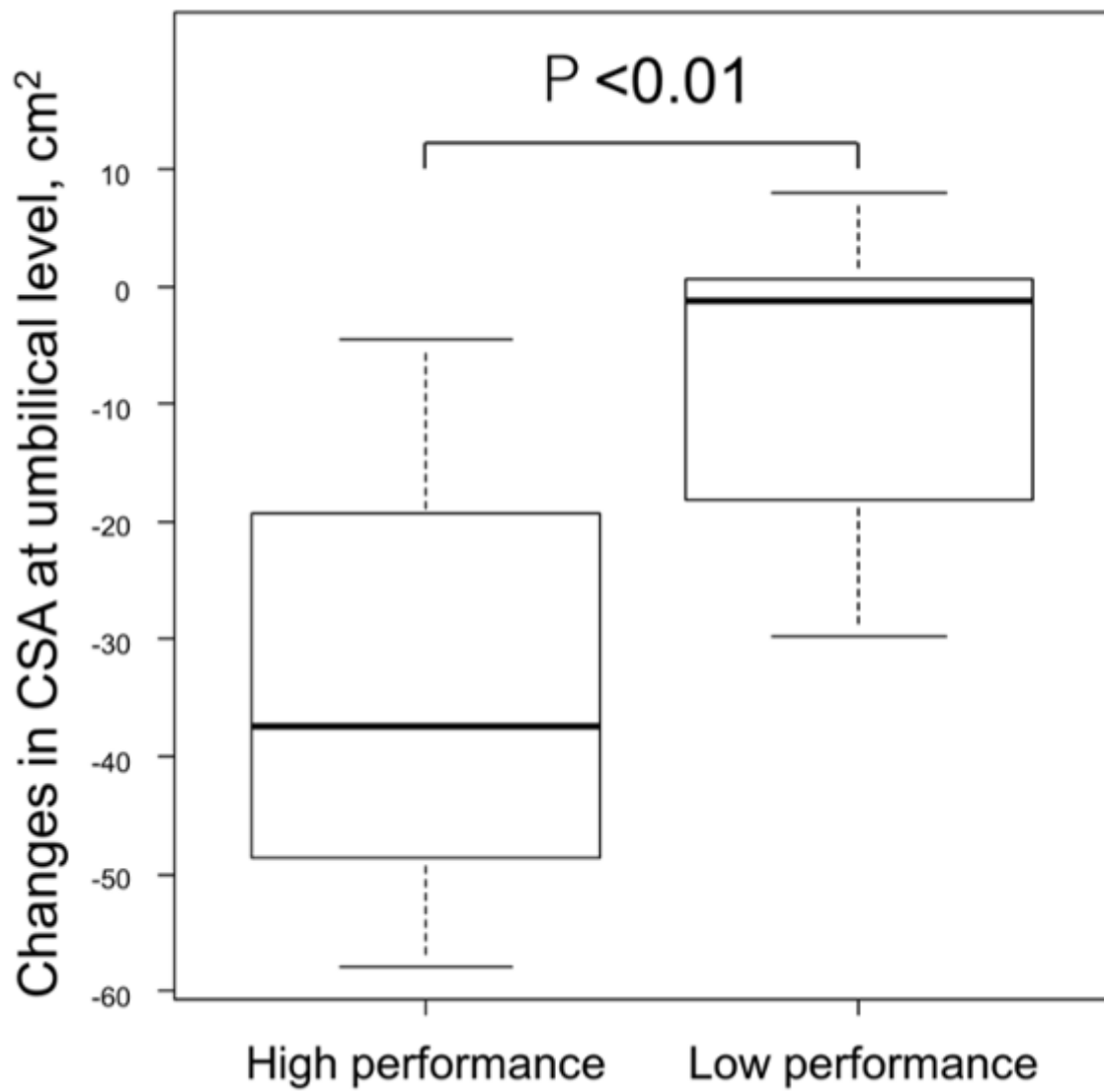


Figure 14

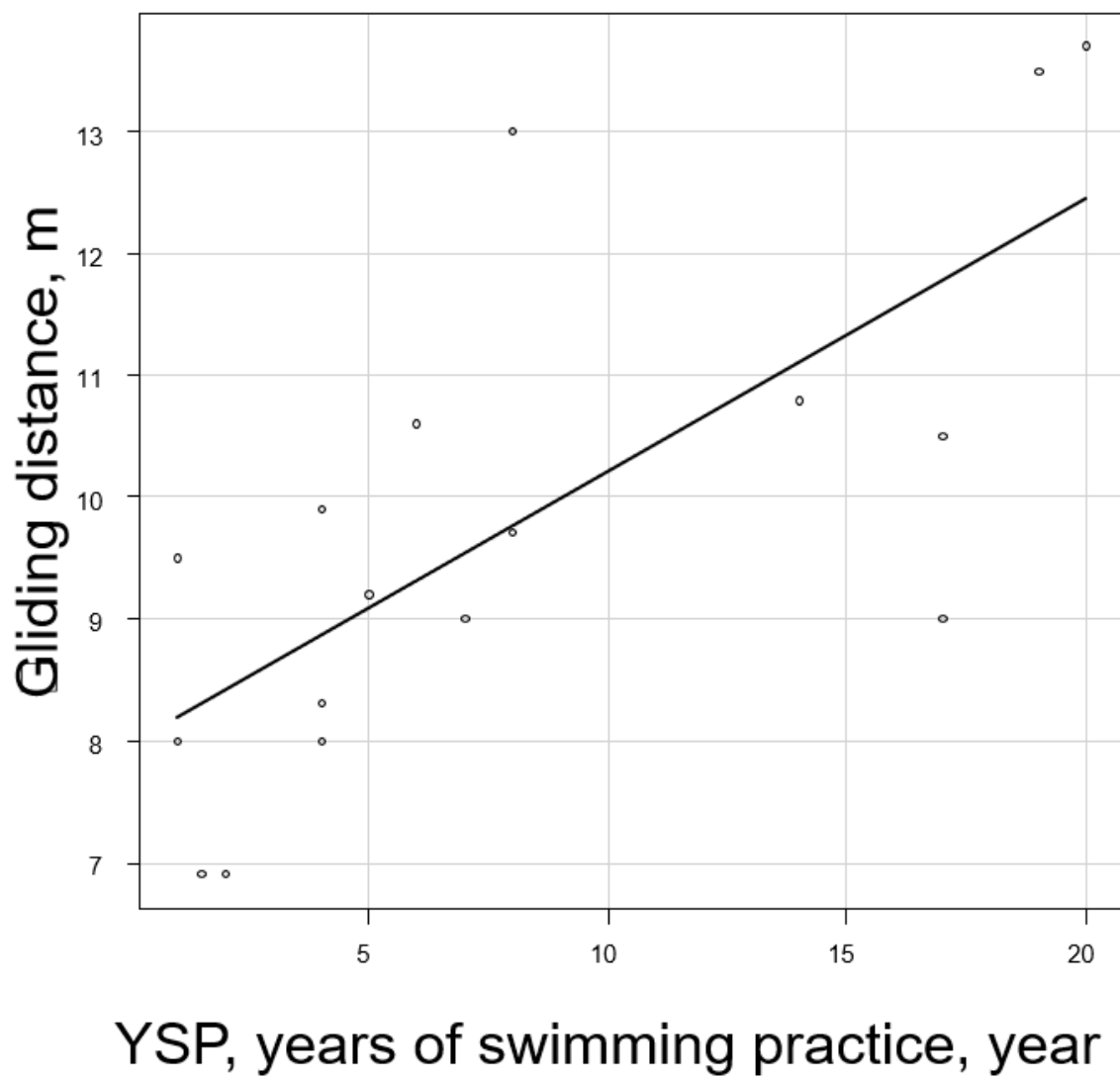


Figure 15

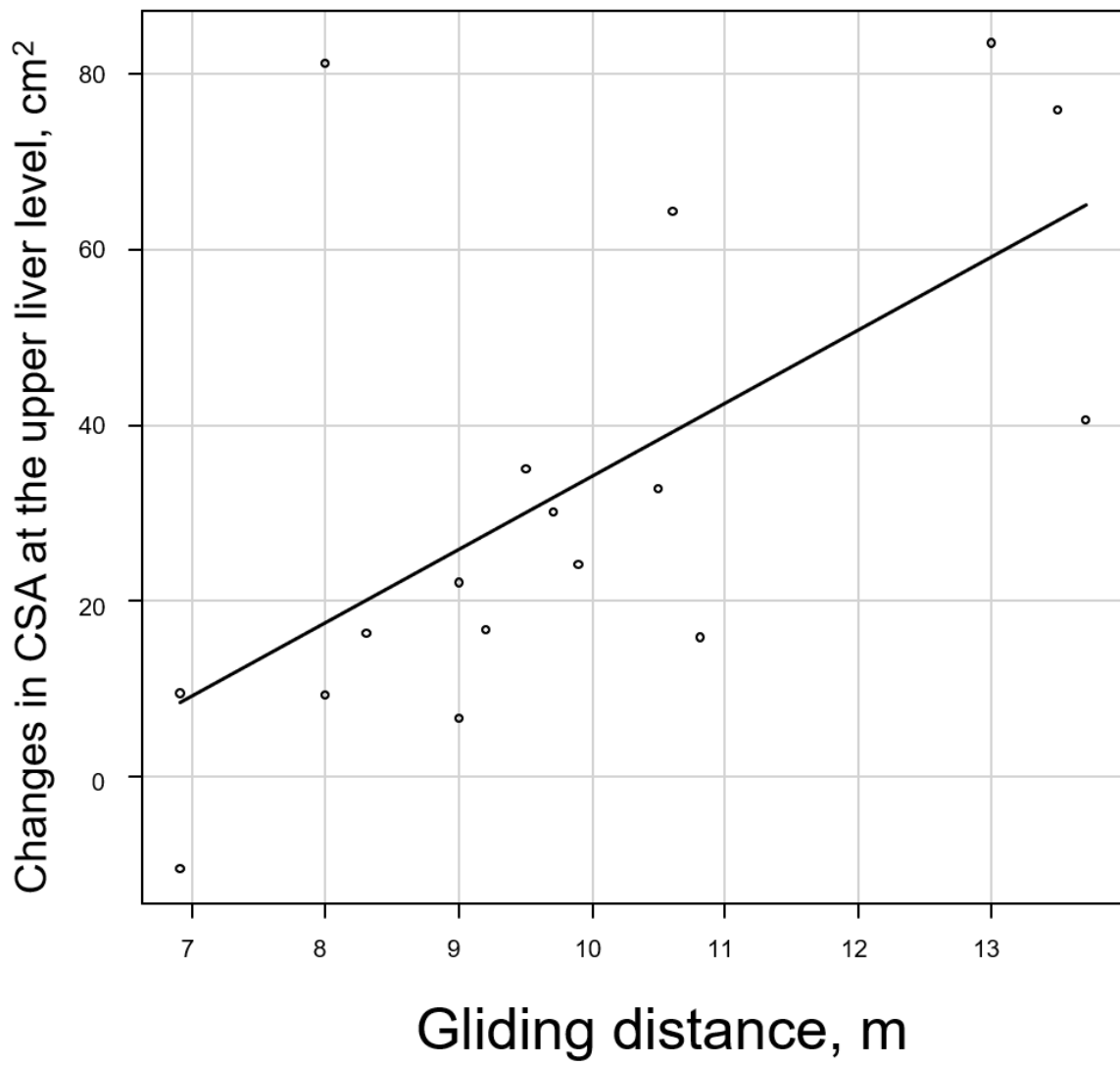


Figure 16

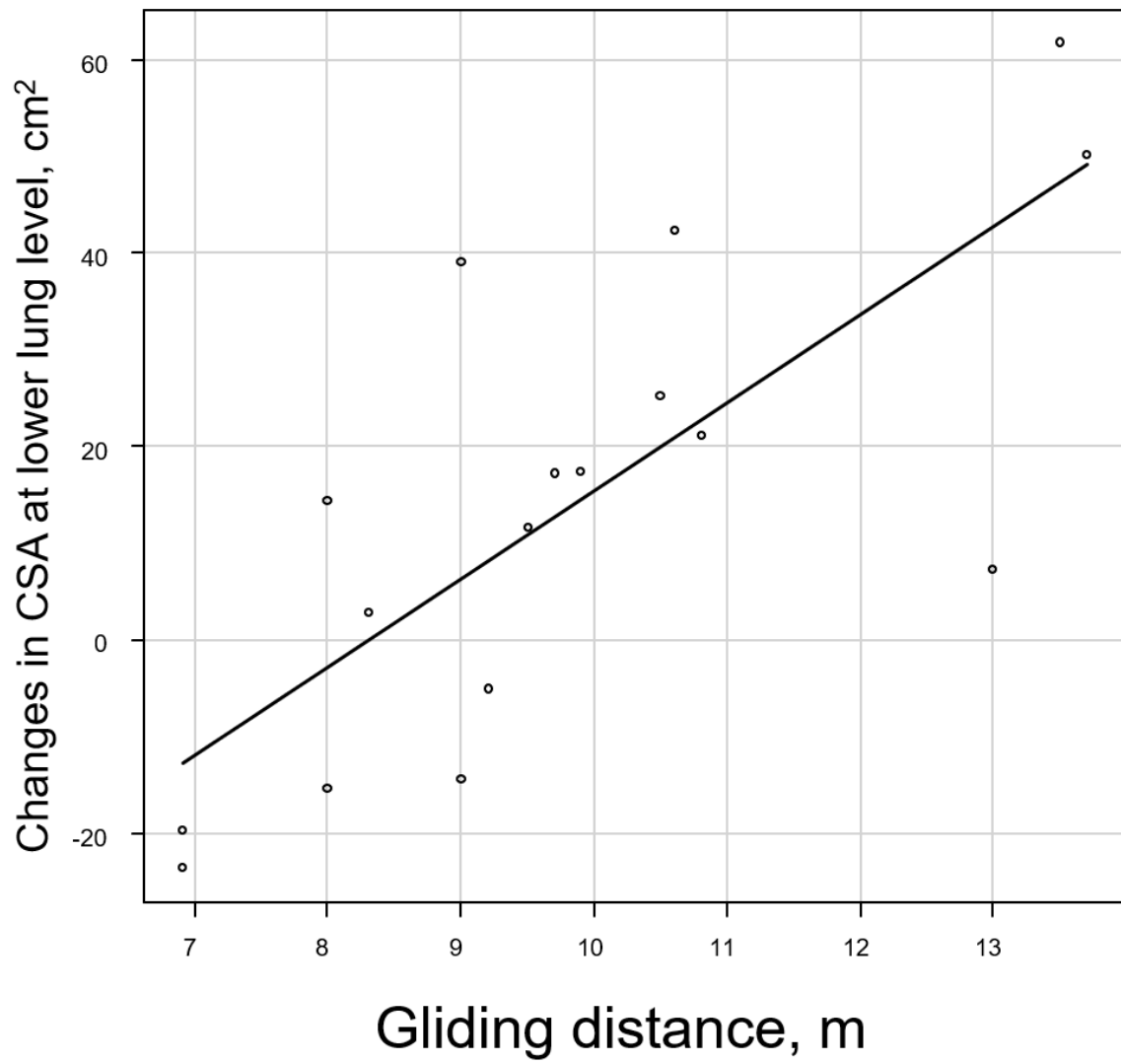


Figure 17

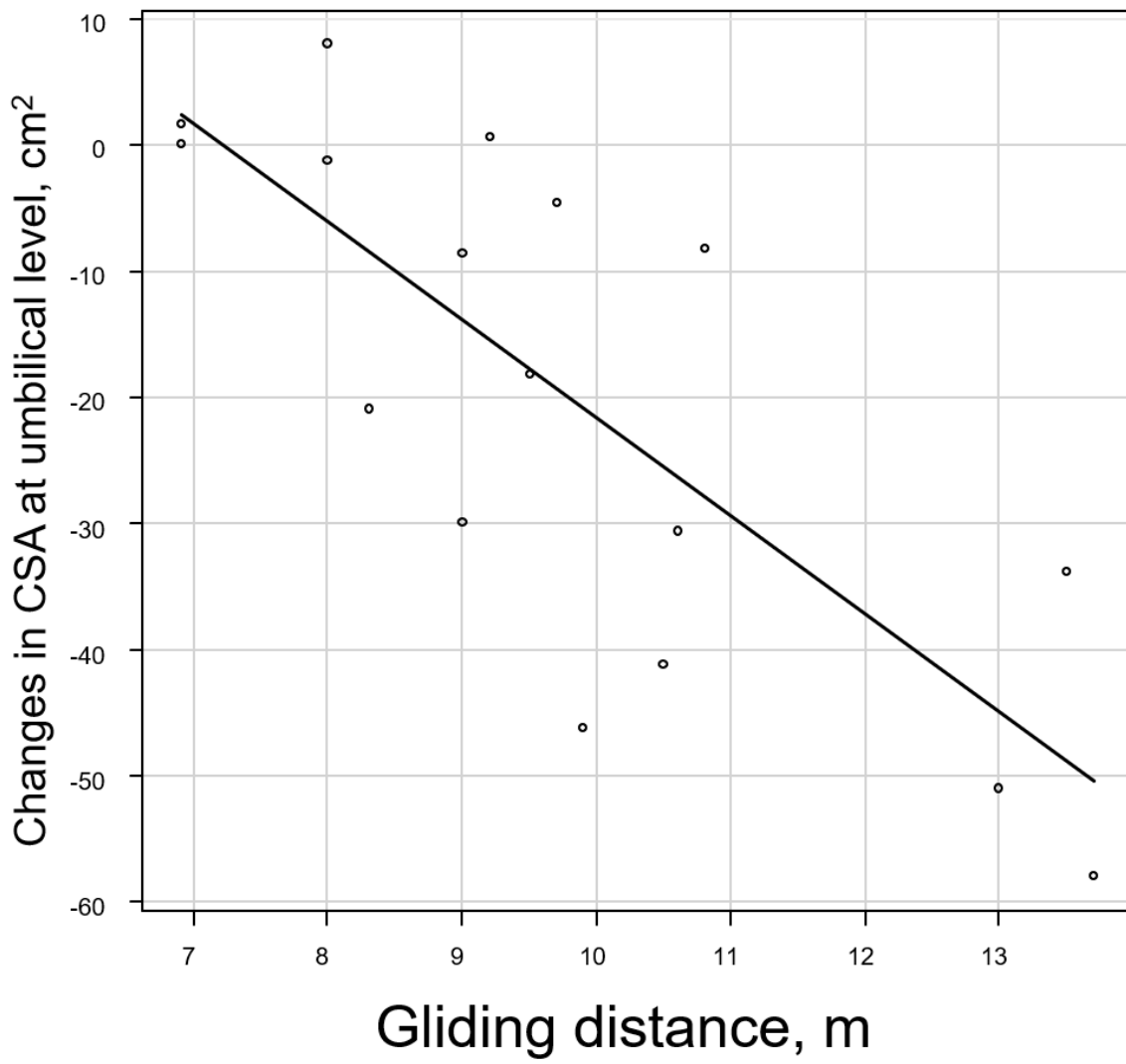


Figure 18

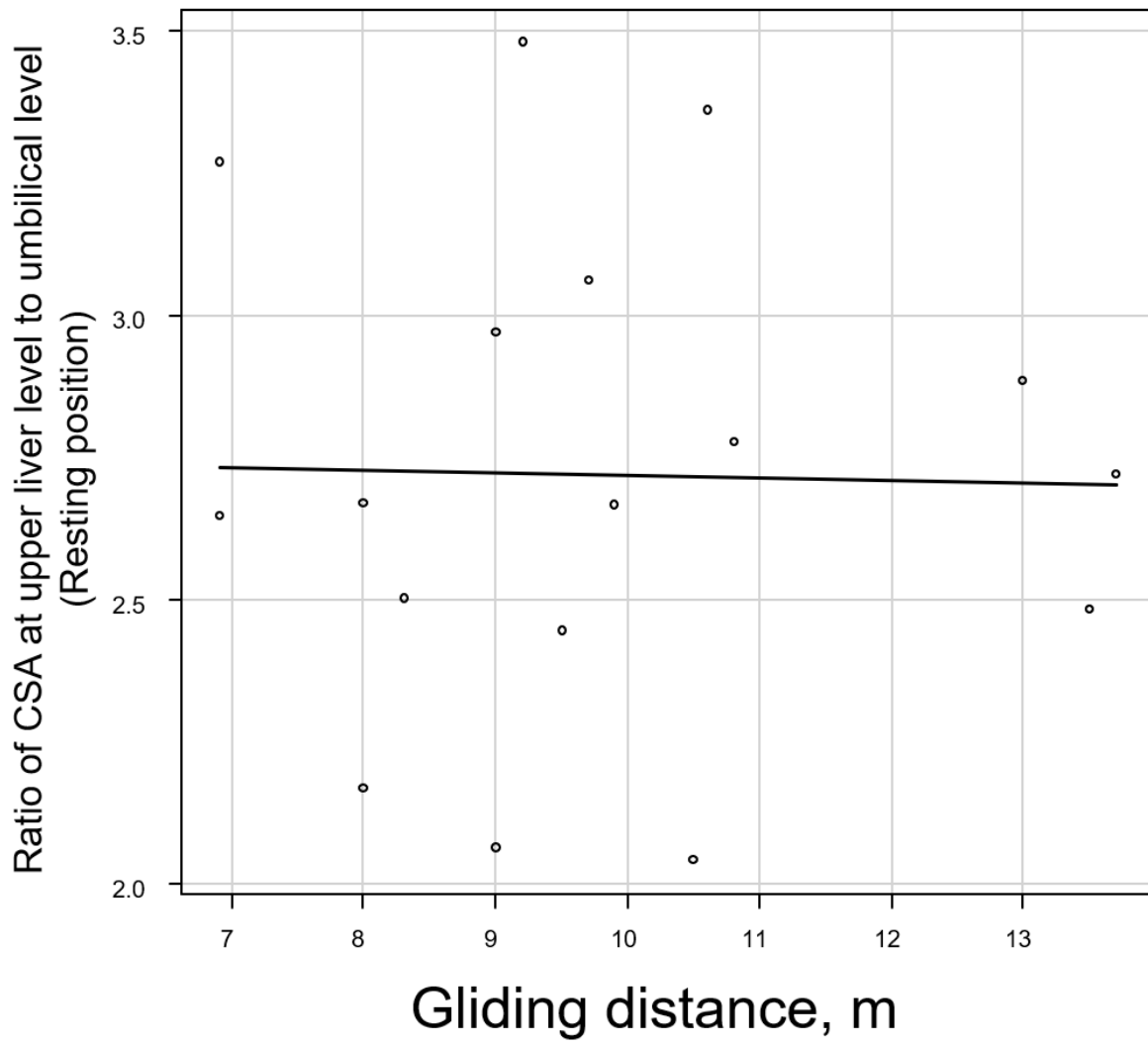


Figure 19

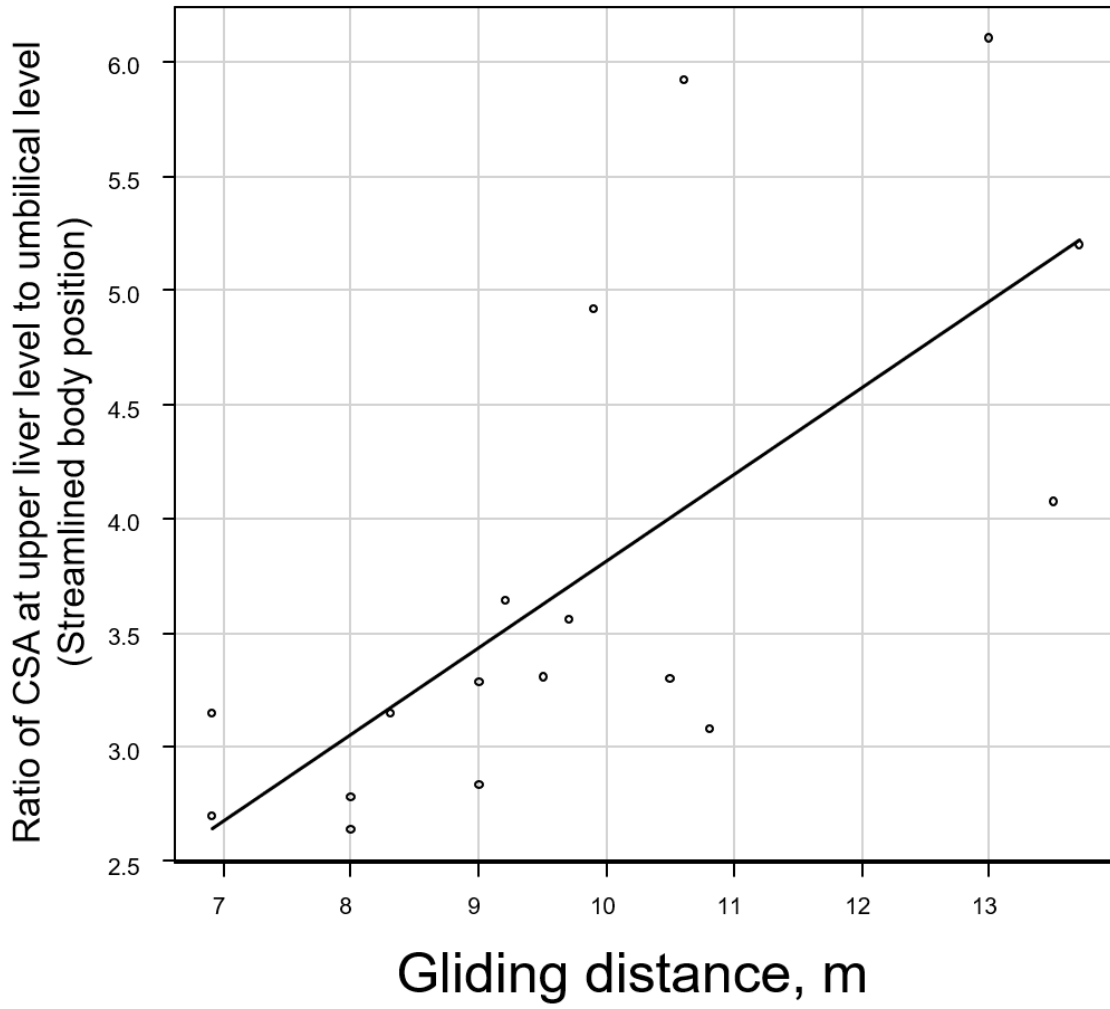


Figure 20

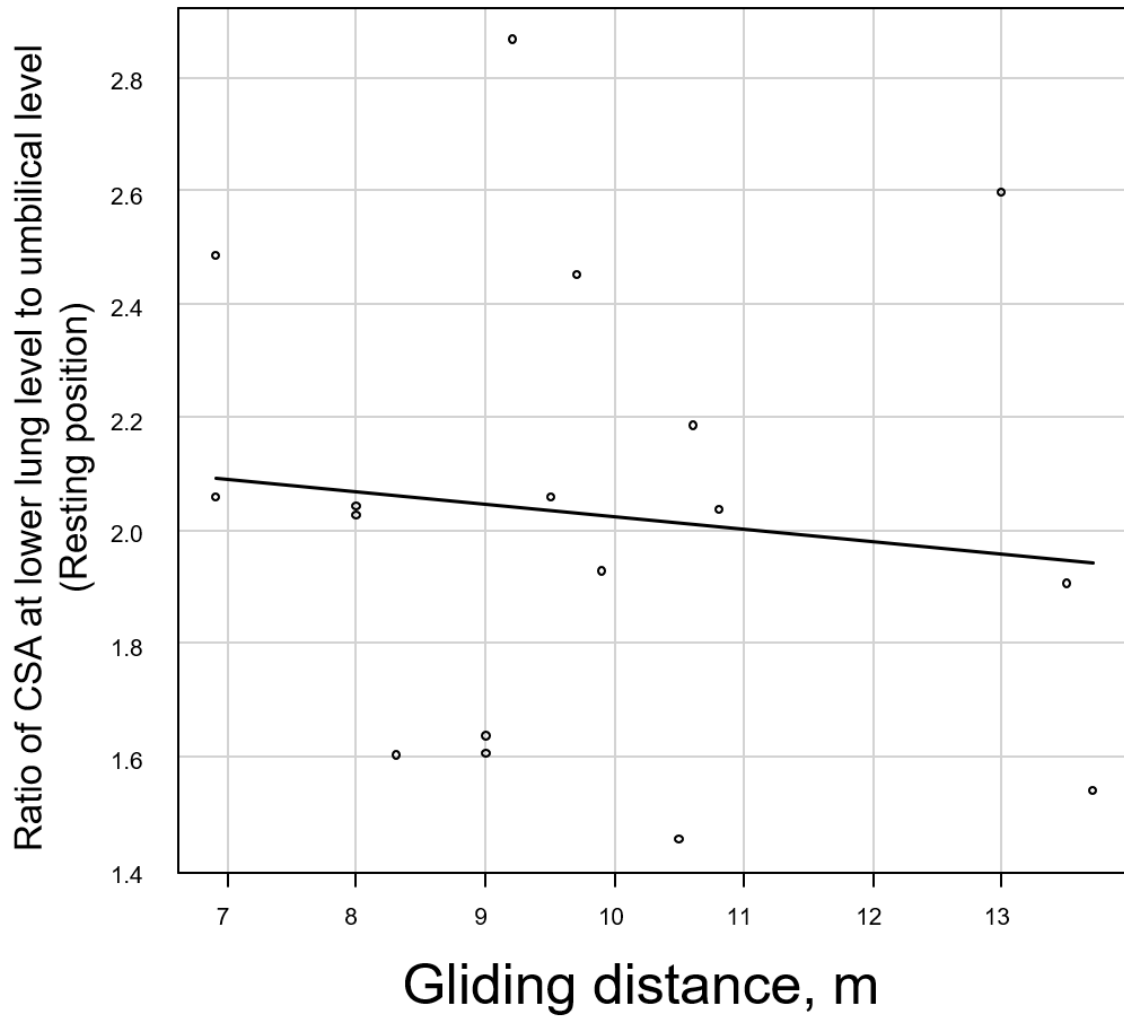


Figure 21

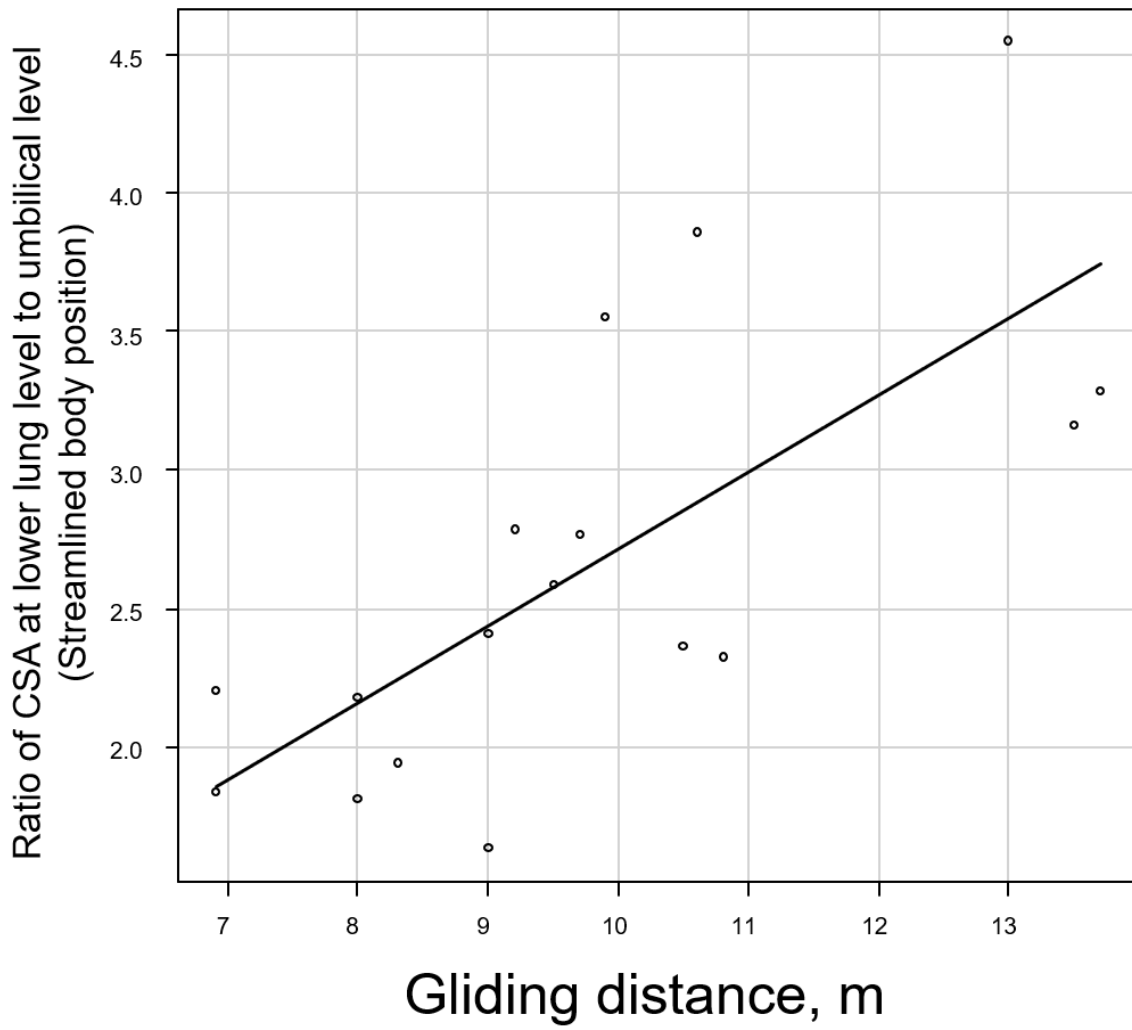


Figure 22

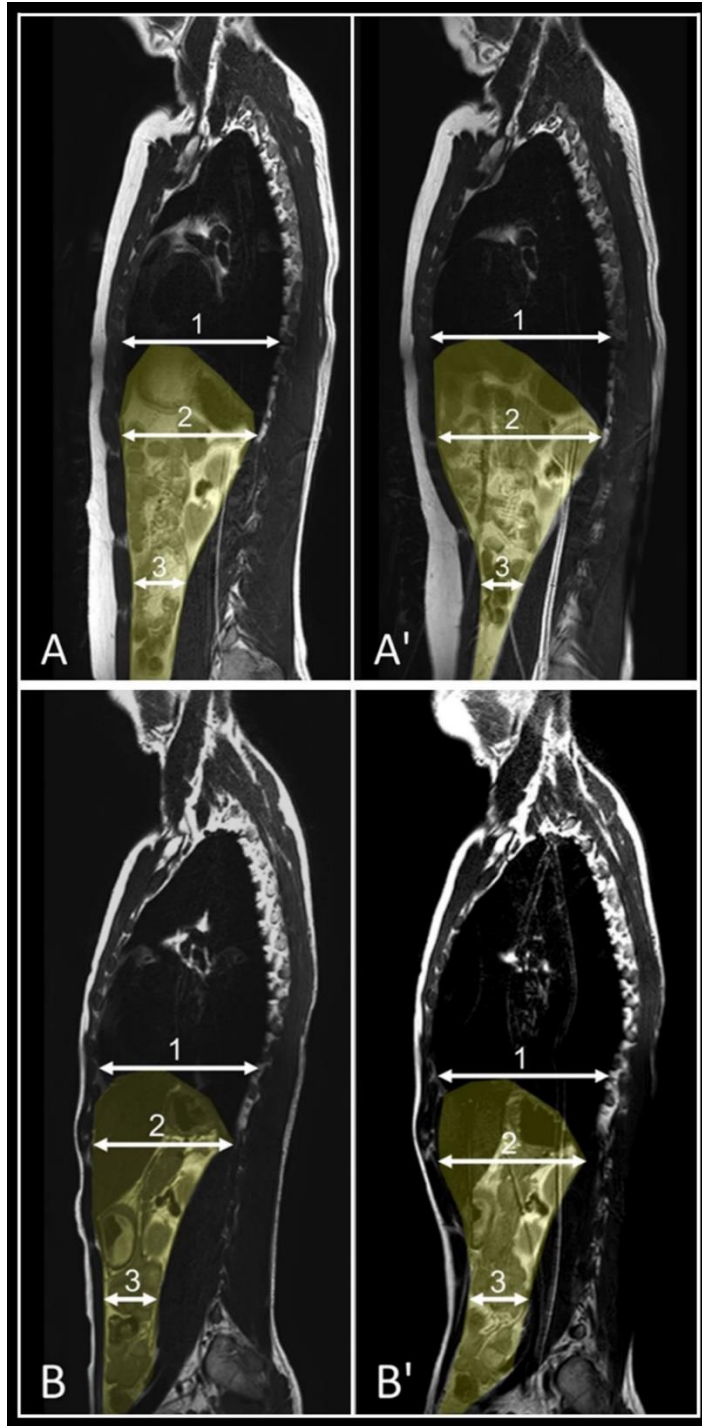


Figure 23

X. Tables

Table 1. Participant characteristics

	High-performance group n = 8	Low-performance group n = 9	<i>P</i> value
Gliding distance (m)	10.7 (10.4–13.1)	8.3 (8.0–9.0)	—
Age (years)	22.0 (21.8–23.0)	22.5 (20.8–23.3)	0.92
YSP (years)	11.0 (7.5–17.5)	4.0 (1.5–5.0)	0.012*
Height (m)	1.73 (1.71–1.77)	1.68 (1.62–1.77)	0.23
Weight (kg)	65.5 (61.5–70.3)	60.0 (52.0–67.0)	0.15
BMI (kg/m ²)	21.1 (20.7–23.3)	20.3 (20.2–21.4)	0.28
BSA	1.78 (1.74–1.83)	1.68 (1.53–1.83)	0.17
Upper limb length (cm)	55.0 (54.5–56.5)	53.0 (50.0–57.0)	0.19
Lower limb length (cm)	89.5 (87.8–91.8)	84.0 (82.0–92.0)	0.25
Shoulder width (cm)	43.5 (42.0–45.0)	42.0 (42.0–43.0)	0.22

All data are presented as medians with interquartile ranges. YSP, years of swimming practice; BMI, body mass index; BSA, body surface area. * $P < 0.05$.

Table 2. Participant characteristics in the measurement of center of gravity

	High-performance group n = 5	Low-performance group n = 5	<i>P</i> value
Gliding distance (m)	10.6 (10.5–10.8)	8.3 (8.0–9.0)	—
Height (m)	1.70 (1.69–1.74)	1.65 (1.61–1.68)	0.059
Length between the tip of the longest finger and the soles of the feet (m)	2.11 (2.09–2.18)	2.04 (2.01–2.10)	0.12
Weight (kg)	68.7 (67.4–73.4)	59.8 (48.8–62.3)	0.032*
BMI (kg/m ²)	22.3 (22.2–24.3)	21.2 (19.1–22.9)	0.22
CGx% (%)	0.334 (0.184–0.359)	0.079 (0.048–0.170)	0.032*

Data are presented as medians with interquartile ranges. CG, distance from the feet to the participant's center of gravity; CGx, movement of the CG from the resting position to the streamlined body position; CGx%, ratio of CGx to the length between the tip of the longest finger and the soles of the feet. * $P < 0.05$.

Table 3. Comparisons of CSA and thickness of the abdominal wall muscle within groups

	Resting position n = 17	Streamlined body position n = 17	<i>P</i> value
CSA at upper liver level (cm²)			
High-performance group	327.3 (294.6–359.7)	392.8 (320.3–410.8)	<0.01**
Low-performance group	285.1 (277.7–308.8)	313.2 (305.4–335.6)	0.027*
CSA at lower lung level (cm²)			
High-performance group	221.6 (211.9–262.0)	257.2 (241.9–306.0)	<0.01**
Low-performance group	221.7 (209.3–230.6)	239.0 (195.9–248.7)	0.65
CSA at umbilical level (cm²)			
High-performance group	128.4 (107.7–135.2)	84.3 (70.2–94.9)	<0.01**
Low-performance group	110.8 (104.9–127.7)	106.6 (92.4–108.4)	0.25
Thickness of rectus abdomen (mm)			
High-performance group	10.2 (9.1–13.0)	10.5 (9.3–14.1)	0.35

Low-performance group	9.2 (7.9–9.4)	9.6 (8.5–11.5)	0.25
-----------------------	---------------	----------------	------

Thickness of TrA + EO + IO

(mm)

High-performance group	20.6 (19.0–21.6)	27.1 (22.2–29.6)	0.016*
------------------------	------------------	------------------	--------

Low-performance group	18.7 (17.2–20.1)	19.6 (18.6–23.8)	0.012*
-----------------------	------------------	------------------	--------

All data are presented as medians with interquartile ranges. CSA, cross-sectional area; TrA, transversus abdominis muscle; EO, external oblique muscle; IO, internal oblique muscle. * $P < 0.05$; ** $P < 0.01$.

Table 4. Changes in CSA from the resting to streamlined body position at three levels between the two groups

	High-performance group n = 17	Low-performance group n = 17	<i>P</i> value
Changes in CSA at the upper liver level (cm ²)	36.8 (28.7 to 67.3)	16.4 (9.3 to 22.2)	0.036*
Changes of CSA at the lower lung level (cm ²)	23.2 (17.3 to 44.2)	-5.1 (-15.4 to 11.6)	<0.01**
Changes in CSA at the umbilical level (cm ²)	-37.4 (-47.4 to -24.9)	-1.2 (-18.1 to 0.75)	<0.01**

All data are presented as medians with interquartile ranges. CSA, cross-sectional area. * $P < 0.05$; ** $P < 0.01$.

Table 5. Correlation between gliding distance and participant characteristics

	Correlation coefficient	
	with gliding distance	<i>P</i> value
	n = 17	
Age (years)	0.17	0.52
YSP (years)	0.74*	<0.01**
Height (m)	0.45	0.070
Weight (kg)	0.55	0.024*
BMI (kg/m ²)	0.36	0.16
BSA	0.52	0.031*
Upper limb length (cm)	0.60	0.011*
Lower limb length (cm)	0.49	0.047*
Shoulder width (cm)	0.44	0.080

The correlation coefficient with gliding distance was measured using Spearman's rank correlation coefficient. YSP, years of swimming practice; BMI, body mass index; BSA, body surface area. *Correlation coefficient > 0.7. *P < 0.05; **P < 0.01.

Table. 6. Correlation between gliding distance and changes in CSA

	Correlation coefficient with gliding	
	distance	<i>P</i> value
	n = 17	
Changes in CSA		
at the upper liver level	0.63	<0.01**
(cm ²)		
Changes in CSA		
at the lower lung level	0.78*	<0.01**
(cm ²)		
Changes in CSA		
at the umbilical level	-0.78*	<0.01**
(cm ²)		

The correlation coefficient with gliding distance was measured using Spearman's rank correlation coefficient. CSA, cross-sectional area. *Correlation coefficient >|0.7|. *P < 0.05; **P < 0.01.

Table. 7. Ratio of CSA at the umbilical level to other CSAs

	High-performance group n = 8	Low-performance group n = 9	<i>P</i> value
Ratio of CSA at the upper liver level to umbilical level (resting position)	2.75 (2.62 to 2.93)	2.65 (2.45 to 2.97)	0.67
Ratio of CSA at the upper liver level to umbilical level (streamlined body position)	4.50 (3.49 to 5.38)	3.15 (2.78 to 3.28)	<0.01**
Ratio of CSA at the lower lung level to umbilical level (resting position)	1.98 (1.81 to 2.25)	2.04 (1.64 to 2.06)	0.74
Ratio of CSA at the lower lung level to umbilical level (streamlined body position)	3.22 (2.67 to 3.63)	2.18 (1.84 to 2.41)	<0.01**

All data are presented as medians with interquartile ranges. CSA, cross-sectional area. * $P < 0.05$; ** $P < 0.01$.

Table. 8. Correlation between gliding distance and the ratio of CSA

	Correlation coefficient with gliding distance n = 17	<i>P</i> value
Ratio of CSA at the upper liver level to umbilical level (resting position)	0.072	0.78
Ratio of CSA at the upper liver level to umbilical level (streamlined body position)	0.78	<0.01**
Ratio of CSA at the lower lung level to umbilical level (resting position)	-0.16	0.55
Ratio of CSA at the lower lung level to umbilical level (streamlined body position)	0.76	<0.01**

Correlation coefficient with gliding distance was measured using Spearman's rank correlation coefficient. CSA, cross-sectional area. * $P < 0.05$; ** $P < 0.01$.